

# **Development of Attrition Resistant Iron-Based Fischer-Tropsch Catalysts**

Final Report

Work Performed Under  
Grant No.: DE-FG26-99FT40619

for

U.S. Department of Energy  
Federal Energy Technology Center  
Pittsburgh, PA 15236

by

Dr. Adeyinka A. Adeyiga  
Department of Chemical Engineering  
Hampton University  
Hampton, VA 23668

December 2003

## DISCLAIMER

This report was prepared as an account of work sponsored by an agency of the United States Government. Neither the United States Government nor any agency thereof, nor any of their employees, makes any warranty, express or implied, or assumes any legal liability or responsibility for the accuracy, completeness, or usefulness of any information, apparatus, product, or process disclosed, or represents that its use would not infringe privately owned rights. Reference herein to any specific commercial product, process, or service by trade name, trademark, manufacturer, or otherwise, does not necessarily constitute or imply its endorsement, recommendation, or favoring by the United States Government or any agency thereof. The views and opinions of authors expressed herein do not necessarily state or reflect those of the United States Government or any agency thereof.

## ABSTRACT

Fischer-Tropsch (FT) synthesis to convert syngas ( $\text{CO} + \text{H}_2$ ) derived from natural gas or coal to liquid fuels and wax is a well-established technology. For low  $\text{H}_2$  to  $\text{CO}$  ratio syngas produced from  $\text{CO}_2$  reforming of natural gas or from gasification of coal, the use of Fe catalysts is attractive because of their high water gas shift activity in addition to their high FT activity. Fe catalysts are also attractive due to their low cost and low methane selectivity. Because of the highly exothermic nature of the FT reaction, there has been a recent move away from fixed-bed reactors toward the development of slurry bubble column reactors (SBCRs) that employ 30 to 90  $\mu\text{m}$  catalyst particles suspended in a waxy liquid for efficient heat removal. However, the use of Fe FT catalysts in an SBCR has been problematic due to severe catalyst attrition resulting in fines that plug the filter employed to separate the catalyst from the waxy product. Fe catalysts can undergo attrition in SBCRs not only due to vigorous movement and collisions but also due to phase changes that occur during activation and reaction.

The objectives of this research were to develop a better understanding of the parameters affecting attrition of Fe F-T catalysts suitable for use in SBCRs and to incorporate this understanding into the design of novel Fe catalysts having superior attrition resistance.

The catalysts were prepared by co-precipitation, followed by binder addition and spray drying at  $250^\circ\text{C}$  in a 1 m diameter, 2 m tall spray dryer. The binder silica content was varied from 0 to 20 wt %.

The results show that use of small amounts of precipitated  $\text{SiO}_2$  alone in spray-dried Fe catalysts can result in good attrition resistance. All catalysts investigated with  $\text{SiO}_2$  wt%  $\leq 12$  produced fines less than 10 wt% during the jet cup attrition test, making them suitable for long-term use in a slurry bubble column reactor. Thus, concentration rather than type of  $\text{SiO}_2$

incorporated into catalyst has a more critical impact on catalyst attrition resistance of spray-dried Fe catalysts. Lower amounts of SiO<sub>2</sub> added to a catalyst give higher particle densities and therefore higher attrition resistances. In order to produce a suitable SBCR catalyst, however, the amount of SiO<sub>2</sub> added has to be optimized to provide adequate surface area, particle density, and attrition resistance.

Two of the catalysts with precipitated and binder silica were tested in Texas A&M University's CSTR (Autoclave Engineers).

Spray-dried catalysts with compositions 100 Fe/5 Cu/4.2 K/11 (P) SiO<sub>2</sub> and 100 Fe/5 Cu/4.2 K/1.1 (B) SiO<sub>2</sub> have excellent selectivity characteristics (low methane and high C<sub>5</sub><sup>+</sup> yields), but their productivity and stability (deactivation rate) need to be improved. Mechanical integrity (attrition strength) of these two catalysts was markedly dependent upon their morphological features. The attrition strength of the catalyst made out of largely spherical particles (1.1 (B) SiO<sub>2</sub>) was considerably higher than that of the catalyst consisting of irregularly shaped particles (11 (P) SiO<sub>2</sub>).

## ACKNOWLEDGEMENTS

This study was sponsored by the U.S. Department of Energy (DOE) under Grant No. DE-FG-26-99FT40619. The authors would like to acknowledge with gratitude the guidance provided by the DOE Contracting Officer's Representatives, Drs. Udaya Rao and Shelby Rogers. The authors also acknowledge the guidance of Süd-Chemie Inc.

Appreciation is also extended to the following people for their guidance and support: Dr. James Goodwin of Clemson University, Dr. Drago Bukur of Texas A&M University, and Dr. K. Jothimurugesan of Conoco-Phillips, Ponca City, Oklahoma.

## TABLE OF CONTENTS

|     |   |    |
|-----|---|----|
| 1.0 | INTRODUCTION .....                                    | 1  |
| 2.0 | EXECUTIVE SUMMARY .....                               | 4  |
| 3.0 | EXPERIMENT .....                                      | 3  |
| 3.1 | Catalyst .....  | 3  |
| 3.2 | Catalyst Characterization .....                       | 4  |
| 4.0 | RESULTS .....   | 6  |
| 4.1 | Catalyst Attrition.....                               | 6  |
| 4.2 | Catalyst Particle Properties .....                    | 9  |
| 4.3 | Catalyst Morphology .....                             | 11 |
| 5.0 | DISCUSSION.....                                       | 16 |
| 5.1 | Catalyst Attrition Resistance.....                    | 16 |
| 5.2 | SiO <sub>2</sub> Structure .....                      | 21 |
| 5.3 | Slurry Reactor Tests.....                             | 23 |
| 5.4 | Catalyst Activity and Selectivity in STSR Tests ..... | 24 |
| 6.0 | CONCLUSION.....                                       | 25 |
|     | LITERATURE REFERENCES .....                           | 34 |
|     | APPENDIX A: Attrition Index Calculations.....         | 38 |
|     | APPENDIX B: FE Reducibility Calculations .....        | 39 |

### List of Figures

|            |   |    |
|------------|---|----|
| Figure 1.  | Jet Cup Attrition Results .....   | 8  |
| Figure 2a. | SEM Micrographs of Fe/P(0) and Fe/P(3) Before and After Attrition .....   | 13 |
| Figure 2b. | SEM Micrographs of Fe/P(5) and Fe/P(8) Before and After Attrition .....   | 14 |
| Figure 2c. | SEM Micrographs of Fe/P(10) and Fe/P(12) Before and After Attrition .....   | 15 |
| Figure 3.  | EDXS Results for the Cross Section of a Typical Fe/P(5) Particle .....  | 17 |
| Figure 4.  | SEM Micrographs of Typical SiO <sub>2</sub> Structures After Acid Leaching<br>[Fe/P(12)]: (a) Typical Structure; (b) Particle with Interior ..... | 18 |

List of Figures (Contd.)

|   |    |
|---|----|
| Figure 5. Weight percentage of Fines Lost vs. Total Concentration of SiO <sub>2</sub> for Different Series of Spray-Dried Fe FT Catalysts ..... | 20 |
| Figure 6. Weight Percentage of Fines Lost vs. Average Particle Density of Calcined Fe/P(y), Fe/B(x), and Fe/P(y)/B(10) catalysts .....          | 22 |
| Figure 7. Syngas Conversion with Time On-Stream for binder Silica .....   | 26 |
| Figure 8. C <sub>1</sub> -C <sub>4</sub> Selectivity with Time on stream for Binder Silica .....  | 27 |
| Figure 9. C <sub>5</sub> + Selectivity with Time on Stream for Binder Silica .....  | 28 |
| Figure 10. Usage Ratio with Time on Stream for Binder Silica .....  | 29 |
| Figure 11. Syngas Conversion with Time On-Stream for Binder Silica .....  | 30 |
| Figure 12. C <sub>1</sub> -C <sub>4</sub> Selectivity with Time On-Stream for Precipitated Silica .....   | 31 |
| Figure 13. C <sub>5</sub> + Selectivity with Time On-Stream for Precipitated Silica .....   | 32 |
| Figure 14. Usage Ratio with Time On-Stream for Precipitated Silica .....  | 33 |

List of Tables

|  |    |
|--|----|
| Table 1. Jet Cup Attrition Results .....   | 7  |
| Table 2. BET Surface Area and Pore Volume of the Iron Catalysts Studied .....    | 10 |
| Table 3. Macro Pore volume and Particle Density of Selected Iron Catalysts ..... | 12 |

# DEVELOPMENT OF ATTRITION RESISTANT IRON-BASED FISCHER-TROPSCH CATALYSTS

## 1.0 INTRODUCTION

Fischer-Tropsch Synthesis (FTS) is the reaction of CO and H<sub>2</sub> (syngas) to form a wide variety of hydrocarbons, typically using iron- or cobalt-based catalysts. Currently there are two commercial FTS plants: SASTECH produces synthetic fuels and chemicals from coal (including recent expansions), and Shell is using FTS to convert natural gas to high value products in Malaysia. There are other units in the planning or construction stage: China plans to make town gas via FTS; Williams Company is constructing a pilot plant to determine the economics of underground coal gasification; and Exxon is evaluating the possibility of locating a large natural gas-based FTS plant in Qatar. These activities clearly show that improvements and innovations in FTS are underway. This process is also strategically important to the U.S. because of its vast coal reserves, and because FTS represents the best means to make high quality transportation fuels and liquid products from coal. In addition to other technical challenges, one of the major problems in control of the reaction is heat removal. Recent progress in this area has focused on the use of a slurry bubble column reactor (SBCR). These reactors offer simple designs and low costs while still permitting high catalyst and reactor productivity. It is generally thought that this will be the reactor of choice for commercial, coal-based FTS in the United States.

Since modern coal gasification plants produce a syngas that is relatively lean in H<sub>2</sub> (H<sub>2</sub>/CO = 0.5-0.7), a catalyst which is active for the FTS reaction ( $\text{CO} + 2 \text{H}_2 \rightarrow \text{-CH}_2\text{-} + \text{H}_2\text{O}$ ) and the water-gas shift (WGS) reaction ( $\text{CO} + \text{H}_2\text{O} \rightarrow \text{CO}_2 + \text{H}_2$ ) is required. The overall reaction on these catalysts is thus  $2\text{CO} + \text{H}_2 \rightarrow \text{-CH}_2\text{-} + \text{CO}_2$ . This allows the efficient use of low H<sub>2</sub>/CO syn gas. Iron-based catalysts, which are active shift catalysts, are thus preferred over cobalt-based catalysts, which are not. Iron is also much less expensive than cobalt.

F-T products are very desirable from an environmental point of view. Because F-T catalysts are very sulfur sensitive, the feed must be completely sulfur free which means that the product is also sulfur free. In addition to being sulfur free, the product is also nitrogen and aromatics free. F-T diesel fuel has a very high cetane number. Although raw F-T naphtha has a



low octane number, it can be processed into high quality gasoline. F-T distillate also makes excellent ethylene plant feedstock.

Catalyst development activities have involved an extensive effort to improve the performance of iron catalysts. Iron catalyst development work has been carried out by the Center for Advanced Energy Research (CAER) and FETC's Office of Science and Technology (OST). These efforts have resulted in iron catalysts with much higher activities than previous catalysts. A problem with iron catalysts is that they tend to have low structural strength with the result that attrition tends to produce very small catalyst particles during slurry operations. This attrition causes plugging, fouling, difficulty in separating the catalyst from the wax product, and loss of the catalyst. This is due to the low attrition resistance of the Fe catalyst and the significant breakage of the Fe particles. Fe catalysts are subject to both chemical as well as physical attrition in a SBCR. Chemical attrition can be caused due to phase changes that any Fe catalyst goes through ( $\text{Fe}_2\text{O}_3 \rightarrow \text{Fe}_3\text{O}_4 \rightarrow \text{FeO} \rightarrow \text{Fe} \rightarrow \text{Fe carbides}$ ) potentially causing internal stresses within the particle and resulting in weakening, spalling or cracking. Physical attrition can result due to collisions between catalyst particles and with reactor wall. Catalyst particles of irregular shapes and non-uniform sizes produced by conventional methods are subject to greater physical attrition.

Another inherent complication associated with the iron-based catalyst is the catalyst pretreatment. Before synthesis, a catalyst precursor is pretreated to convert the catalyst into an active form. The pretreatment of Fe is not as straight forward as that for Ru, Co or Ni. Although pretreatment includes reduction of the iron particles, other processes are also involved. The pretreatment of iron FT catalysts is not clearly understood. Part of the confusion stems from the fact that the nature and composition of iron catalysts change during reaction. These changes depend on the temperature, time of exposure to the reactant feed, nature of the reactor system, and composition of the feed, and activation conditions (time and temperature). The common pretreatment conditions employed in the case of iron catalysts are  $\text{H}_2$  reduction, CO reduction (and carbiding), or reduction in the reactant syngas. Work at the Federal Energy Technology Center has focused on the effect of catalyst pretreatment and the impact of the liquid starting medium on syngas conversion in a stirred tank slurry reactor.

Several phases of iron are known to exist when iron-based catalysts are subjected to F-T synthesis conditions. These include metallic iron ( $\alpha$ -Fe), iron oxides (hematite,  $\alpha$ - $\text{Fe}_2\text{O}_3$ ;

magnetite,  $\text{Fe}_3\text{O}_4$  and  $\text{Fe}_x\text{O}$ ), and iron carbides, of which at least five different forms are known to exist. These include O-carbides (carbides with carbon atoms in octahedral interstices,  $\epsilon\text{-Fe}_2\text{C}$ ,  $\epsilon'\text{-Fe}_{2.2}\text{C}$ , and  $\text{Fe}_x\text{C}$ ) and TP-carbides (carbides with carbon atoms in trigonal prismatic interstices,  $\chi\text{-Fe}_{2.5}\text{C}$  and  $\text{Fe}_3\text{C}$ ). The formation and distribution of these phases depend on the reaction conditions, reaction times, and state of the catalyst (reduced/unreduced, supported/unsupported, etc.). However, the role of each of these phases during the reaction has not been resolved.

Potassium and copper are typically used as chemical promoters for iron FT catalysts. The adsorption of CO on iron results in a net withdrawal of electrons from the metal, whereas hydrogen adsorption tends to donate electrons to the metal. Potassium and the associated  $\text{O}^{2-}$  donate electrons to the metal, enhancing CO adsorption while weakening  $\text{H}_2$  adsorption. This leads to decreased hydrogenation and increased chain growth during the synthesis reaction, yielding higher molecular weight products (i.e., a higher  $\alpha$ ). More lower olefins are also produced. Potassium also decreased  $\text{CH}_4$  production and increases WGS activity. Copper on the other hand is introduced to facilitate reduction of the iron itself. Copper is more effective in increasing the FTS reaction rate than potassium. Also the average molecular weight is increased in the presence of copper.

The objective of this research is to develop robust iron-based Fischer-Tropsch catalysts that have suitable activity, selectivity and stability to be used in the slurry bubble column reactor. Specifically we aim to develop to: (i) improve the performance and preparation procedure of the high activity, high attrition resistant, high alpha iron-based catalysts synthesized at Hampton University, (ii) seek improvements in the catalyst performance through variations in process conditions, pretreatment procedures and/or modification in catalyst preparation steps and (iii) investigate the performance in a slurry reactor.

## 2.0 EXECUTIVE SUMMARY

Fischer-Tropsch (FT) synthesis to convert syngas ( $\text{CO} + \text{H}_2$ ) derived from natural gas or coal to liquid fuels and wax is a well-established technology. For low  $\text{H}_2$  to  $\text{CO}$  ratio syngas produced from  $\text{CO}_2$  reforming of natural gas or from gasification of coal, the use of Fe catalysts is attractive because of their high water gas shift activity in addition to their high FT activity. Fe catalysts are also attractive due to their low cost and low methane selectivity. Because of the highly exothermic nature of the FT reaction, there has been a recent move away from fixed-bed reactors toward the development of slurry bubble column reactors (SBCRs) that employ 30 to 90  $\mu\text{m}$  catalyst particles suspended in a waxy liquid for efficient heat removal. However, the use of Fe FT catalysts in an SBCR has been problematic due to severe catalyst attrition resulting in fines that plug the filter employed to separate the catalyst from the waxy product. Fe catalysts can undergo attrition in SBCRs not only due to vigorous movement and collisions but also due to phase changes that occur during activation and reaction.

The objectives of this research were to develop a better understanding of the parameters affecting attrition of Fe F-T catalysts suitable for use in SBCRs and to incorporate this understanding into the design of novel Fe catalysts having superior attrition resistance.

The catalysts were prepared by co-precipitation, followed by binder addition and spray drying at  $250^\circ\text{C}$  in a 1 m diameter, 2 m tall spray dryer. The binder silica content was varied from 0 to 20 wt %.

The results show that use of small amounts of precipitated  $\text{SiO}_2$  alone in spray-dried Fe catalysts can result in good attrition resistance. All catalysts investigated with  $\text{SiO}_2$  wt%  $\leq 12$  produced fines less than 10 wt% during the jet cup attrition test, making them suitable for long-term use in a slurry bubble column reactor. Thus, concentration rather than type of  $\text{SiO}_2$  incorporated into catalyst has a more critical impact on catalyst attrition resistance of spray-dried Fe catalysts. Lower amounts of  $\text{SiO}_2$  added to a catalyst give higher particle densities and therefore higher attrition resistances. In order to produce a suitable SBCR catalyst, however, the amount of  $\text{SiO}_2$  added has to be optimized to provide adequate surface area, particle density, and attrition resistance.

Two of the catalysts with precipitated and binder silica were tested in Texas A&M University's CSTR (Autoclave Engineers).

Spray-dried catalysts with compositions 100 Fe/5 Cu/4.2 K/11 (P)  $\text{SiO}_2$  and 100 Fe/5 Cu/4.2 K/1.1 (B)  $\text{SiO}_2$  have excellent selectivity characteristics (low methane and high  $\text{C}_5^+$  yields), but their productivity and stability (deactivation rate) need to be improved. Mechanical integrity (attrition strength) of these two catalysts was markedly dependent upon their morphological features. The attrition strength of the catalyst made out of largely spherical particles (1.1 (B)  $\text{SiO}_2$ ) was considerably higher than that of the catalyst consisting of irregularly shaped particles (11 (P)  $\text{SiO}_2$ ).

## 3.0 EXPERIMENT

### 3.1 Catalyst

A series of spray-dried Fe FT catalysts having compositions of 100/Fe/5Cu/4.2K/  $x$ SiO<sub>2</sub> was used in this study. Six catalyst composition in this series were prepared with precipitated SiO<sub>2</sub> at different levels: 0, 3, 5, 8, 10, and 12 wt% based on total catalyst weight. Fe/P( $y$ ) is used to refer to each catalyst composition according to its precipitated SiO<sub>2</sub> content incorporated; for instance, Fe/P(5) refers to the catalyst composition with 5 wt% precipitated SiO<sub>2</sub> added. The concentrations of Cu and K relative to Fe remained identical for all catalyst compositions; therefore, they are not used in the catalyst nomenclature. The details of catalyst preparation can be found elsewhere. In brief, a solution containing the desired ratio of Fe(NO<sub>3</sub>)<sub>3</sub> • 9 H<sub>2</sub>O, Cu(NO<sub>3</sub>)<sub>2</sub> • 2.5 H<sub>2</sub>O, and Si(OC<sub>2</sub>H<sub>5</sub>)<sub>4</sub> (added to give precipitated SiO<sub>2</sub>) was precipitated with ammonium hydroxide. An aqueous potassium promoter KHCO<sub>3</sub> was added to a slurry of the precipitate. The slurry was spray-dried at 250°C in a Niro spray drier and was then calcined at 300°C for 5 hours in a muffle furnace. The calcined catalysts were sieved between 38-90 µm before attrition testing and other characterizations.

### 3.2 Catalyst Characterization

Attrition tests were conducted using a jet cup system. The details of the system configuration as well as test procedure have been extensively described previously. In the jet cup test, 5g of each calcined catalyst sample was evaluated for attrition resistance under identical testing conditions using an air jet flow of 15 l/min with a relative humidity of 60 ±5% at room temperature and atmospheric pressure. After one hour time-on-stream, the air jet flow was stopped and the weight of fines collected by the downstream filter was determined. “Weight percentage of fines lost” was calculated and used as one of the attrition indices. Particle size distribution before and after attrition testing was determined with a Leeds & Northrup Microtrac laser particle size analyzer and used to calculate “net change in volume moment”, the other attrition index used in our attrition studies. Volume moment is a measure of the average particle size.

A Philips XL30 Scanning Electron Microscope (SEM) was used to observe the morphology of the catalyst particles, before and after attrition, and also the structure of the precipitated SiO<sub>2</sub> network in the catalyst particles, after acid leaching. Elemental analysis was carried out to determine surface composition and distribution of each element on cross-sectional

surfaces of catalyst particles using Energy Dispersive X-ray Spectroscopy (EDXS). Powder XRD patterns of the catalyst samples was determined using a Philips X'pert Diffractometer. Catalyst BET surface areas and pore volumes were measured using a Micromeritics ASAP 2010 automated system. Each catalyst sample was degassed under vacuum at 100°C for one hour and then 300°C for three hours before BET surface area and pore volume measurements. Average particle density (particle mass divided by its volume) of each catalyst was determined using low-pressure mercury intrusion.

## 4.0 RESULTS

### 4.1 Catalyst Attrition

Attrition results for all the catalysts studied are summarized in Table 1 and the plot of the two attrition indices, “weight percentage of fines lost” and “net change in volume moment” versus total silica concentration is shown in Figure 1. Weight percentage of fines lost was calculated based on the ratio of the weight of fines collected from the exit filter of the jet cup and the total weight of all particles recovered after the jet cup test. Net change in volume moment average particle size change during the attrition test. Since the average particle size decreases during attrition, net change in volume moment is always a positive number. Volume moments of the attritted catalysts were calculated based on both fines generated and particles remaining in the jet cup. Therefore, net change in volume moment is calculated by  $\{[\text{volume moment of fresh} - \text{volume moment of attritted (average bottom and fines)}] / [\text{volume moment of fresh}]\} \times 100$ . Detailed calculations and significance of attrition indices have been given elsewhere. High values of attrition indices indicate low attrition resistances of catalysts.

As shown in Figure 1, the catalyst without precipitated SiO<sub>2</sub> (Fe/P(0)) showed the highest attrition resistance (least attrition) among all the catalysts tested, while the lowest attrition resistance (highest attrition) was exhibited by the catalysts with the highest concentration of precipitated SiO<sub>2</sub>. Figure 1 shows clearly that both attrition indices had similar trends with varying concentration of precipitated SiO<sub>2</sub>. Effect of fluidization differences (as a result of particle density differences) on catalyst attrition in the jet cup has been considered and proved to be negligible by using an ultrasonic attrition test, an attrition test with no fluidization involved. Attrition results from the ultrasonic test were found to be comparable and reproducible within experimental error to those obtained with the jet cup test.

Table 1. Jet Cup Attrition Results

| Catalyst | Total SiO <sub>2</sub><br>Concentration (wt%) | Fines Lost (wt%) <sup>(a,b)</sup> | Net Change in Volume<br>Moment (5) <sup>(c,d,e)</sup> |
|----------|---|-----------------------------------|---|
| Fe/P(0)  | 0.0   | 3.2                               | 6.0   |
| Fe/P(3)  | 2.7   | 6.4                               | 18.4  |
| Fe/P(5)  | 5.2   | 7.5                               | 23.4  |
| Fe/P(8)  | 7.6   | 8.6                               | 27.1  |
| Fe/P(10) | 9.9   | 9.3                               | 30.1  |
| Fe/P(12) | 12.1  | 7.7                               | 27.8  |
| Fe/P(16) | 16.1  | 24.5                              | --  |
| Fe/P(20) | 19.8  | 29.9                              | --  |

(a) Wt% fines = weight of fines collected/weight of total catalyst recovered x 100%

(b) Error =  $\pm 10\%$  of the value measured.

(c) Net change in volume moment was determined with reference to the particle size distribution before attrition testing.

(d) Net change in volume moment (VM) = [(VM of sample after attrition test – VM of sample before test) / VM of sample before test] x 100%.

(e) Error =  $\pm 5\%$  of the value measured.

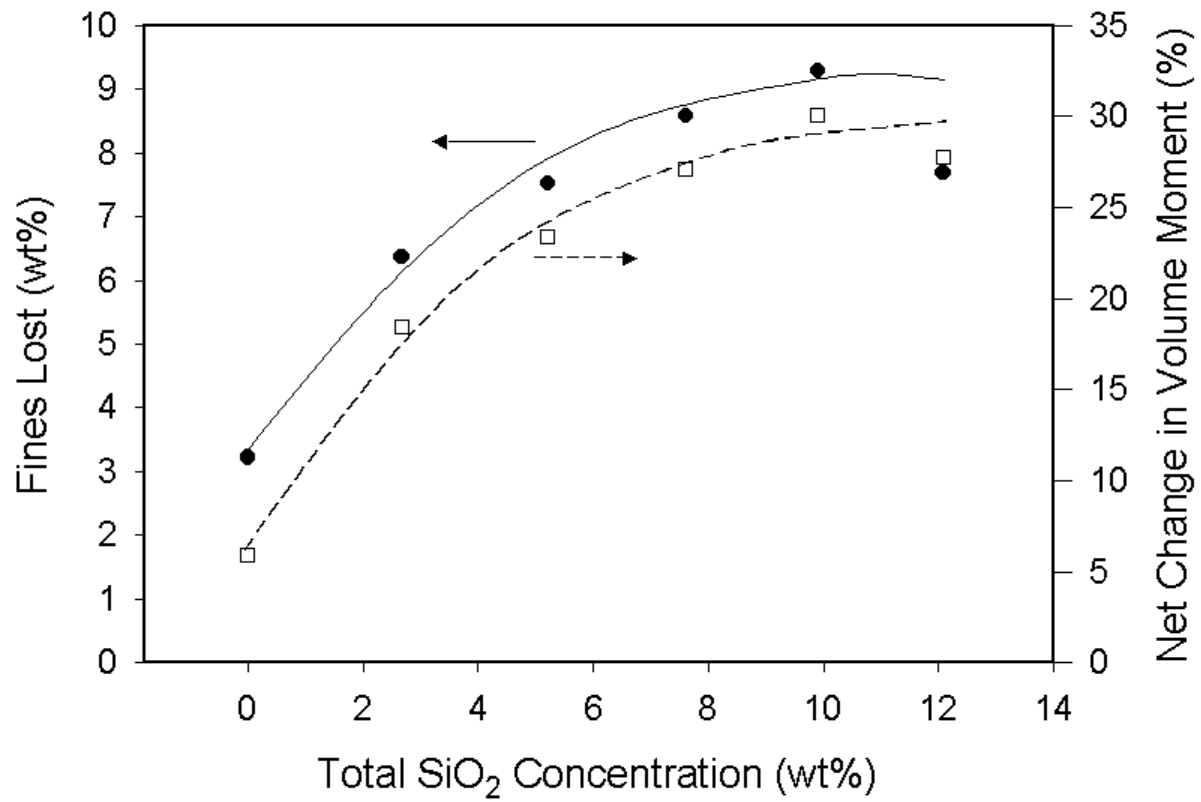


Figure 1. Jet Cup Attrition Results

## 4.2 Catalyst Particle Properties

The BET surface areas and pore volumes (micro- and meso-pores) of the catalysts, measured by N<sub>2</sub> physisorption, are summarized in Table 2. It can be seen (Table 2) that BET surface areas fluctuated with the total concentration of SiO<sub>2</sub>, and no relationship between these two parameters can be drawn. It should be noted that the experimental error of BET surface area measurement is  $\pm 5\%$  based on multiple runs of the same sample. However, this error is increased to ca.  $\pm 10\%$  by an added sampling error due to potential partial segregation of different particle sizes and densities within a powder sample. In addition, surface area of catalysts may fluctuate somewhat due to slight variations in a number of preparation parameters (especially precipitation pH). As expected, the catalyst with 0% SiO<sub>2</sub> had the lowest BET surface area. However, BET surface areas of all the catalysts tested did not change significantly during attrition, except for Fe/P(5) and Fe/P(8). The pore volumes of this catalyst series did not vary significantly with total SiO<sub>2</sub> content and remained essentially unchanged after attrition.

The XRD patterns of all the catalysts tested before and after attrition were found to be identical and confirmed that iron existed mainly as hematite (Fe<sub>2</sub>O<sub>3</sub>). Other components including precipitated SiO<sub>2</sub> were not detectable. The attrition process did not change the XRD patterns of hematite significantly. Thus, as to be expected, attrition affected only physical properties of the catalyst particles and not chemical ones.

Particle density (particle mass divided by its volume including all pore volumes) has been suggested to strongly govern attrition resistance of our spray-dried Fe FT catalysts in calcined, reduced, and carburized forms. Particle density was determined based on low-pressure mercury intrusion in order to prevent mercury from penetrating into the pores of the particles. Mercury porosimetry was used to measure macro pore volumes of the catalyst samples. Particle density and macro pore volume results are summarized in Table 3. It can be seen that macro pore volumes of the selected samples were essentially similar within experimental error. The catalyst with no precipitated SiO<sub>2</sub> (Fe/P(0)) had the highest particle density. Particle density decreased as the concentration of precipitated SiO<sub>2</sub> increased.



Table 2. BET Surface Area and Pore Volume of the Iron Catalysts Studied.

| Catalyst | BET Surface Area (m <sup>2</sup> /g) <sup>(a)</sup> |           | Pore Volume (cm <sup>3</sup> /g) <sup>(b)</sup> |           |
|----------|---|-----------|---|-----------|
|          | Fresh   | Attritted | Fresh   | Attritted |
| Fe/P(0)  | 24  | 23        | 0.08  | 0.08      |
| Fe/P(3)  | 69  | 63        | 0.12  | 0.11      |
| Fe/P(5)  | 83  | 115       | 0.12  | 0.16      |
| Fe/P(8)  | 48  | 69        | 0.11  | 0.14      |
| Fe/P(10) | 41  | 44        | 0.11  | 0.11      |
| Fe/P(12) | 76  | 84        | 0.11  | 0.12      |

(a) Error =  $\pm 5\%$  of the value measured.

(b) Error =  $\pm 10\%$  of the value measured.

### 4.3 Catalyst Morphology

SEM micrographs of all the catalyst samples before and after attrition are shown in Figures 2A-C. The catalyst with no precipitated SiO<sub>2</sub> (Figure 2A/Top) shows clearly non-spherical particles while the other catalysts with addition of precipitated SiO<sub>2</sub> have particles somewhat more rounded in shape and agglomerated. The figures show that breakage during attrition was mostly a break up of particle agglomerates since there was an obvious decrease in numbers of agglomerates after attrition. There was no evidence for the actual breakage of distinct catalyst particles. The presence of small chips and pieces caused by abrasion was observed in the fines collected at the top exit of the jet cup. Degree of breakage increased as the amount of precipitated SiO<sub>2</sub> incorporated increased, which is in good agreement with changes in the attrition indices. It can also be observed that some particles had interior holes, seen only as dark spots on particles at higher magnification in Figures 2A-C. Such holes, which have also been found for the spray-dried Fe catalysts studied previously, were probably produced because of the lower efficiency of a laboratory scale spray drier. Only a small minority of these catalyst particles had holes but they provided a means to determine if the silica structure was maintained during acid leaching of the catalyst particles, discussed in detail later.

To obtain a better understanding of the factors affecting attrition resistance, catalyst inner structure as well as distribution of each element in the catalyst particles are important to determine. The distribution of each element in the catalyst particles was determined using EDXS to analyze the cross-sectional area of catalyst particles prepared by microtoming. The elemental mapping results, an example being shown in Figure 3, were found to be similar for all catalyst compositions containing precipitated SiO<sub>2</sub>. Iron, Cu and precipitated SiO<sub>2</sub> were found to be evenly distributed throughout the catalyst particles. Potassium, on the other hand, was found in higher concentration at catalyst surfaces as seen on the outer edge of the cross-sectioned particles.

Table 3. Macro Pore Volume and Particle Density of Selected Iron Catalysts.

| Catalyst | Macro Pore Volume (cm <sup>3</sup> /g) <sup>(a)</sup> | Particle Density (g/cm <sup>3</sup> ) <sup>(b)</sup> |
|----------|---|--|
| Fe/P(0)  | 0.25  | 1.64   |
| Fe/P(10) | 0.26  | 1.40   |
| Fe/P(12) | 0.24  | 1.44   |
| Fe/P(16) | --  | 0.81   |
| Fe/P(20) | --  | 0.79   |

(a) Measured using mercury porosimetry, error =  $\pm 10\%$  of the value measured.

(b) Determined using low-pressure mercury displacement, error =  $\pm 5\%$  of the value measured.

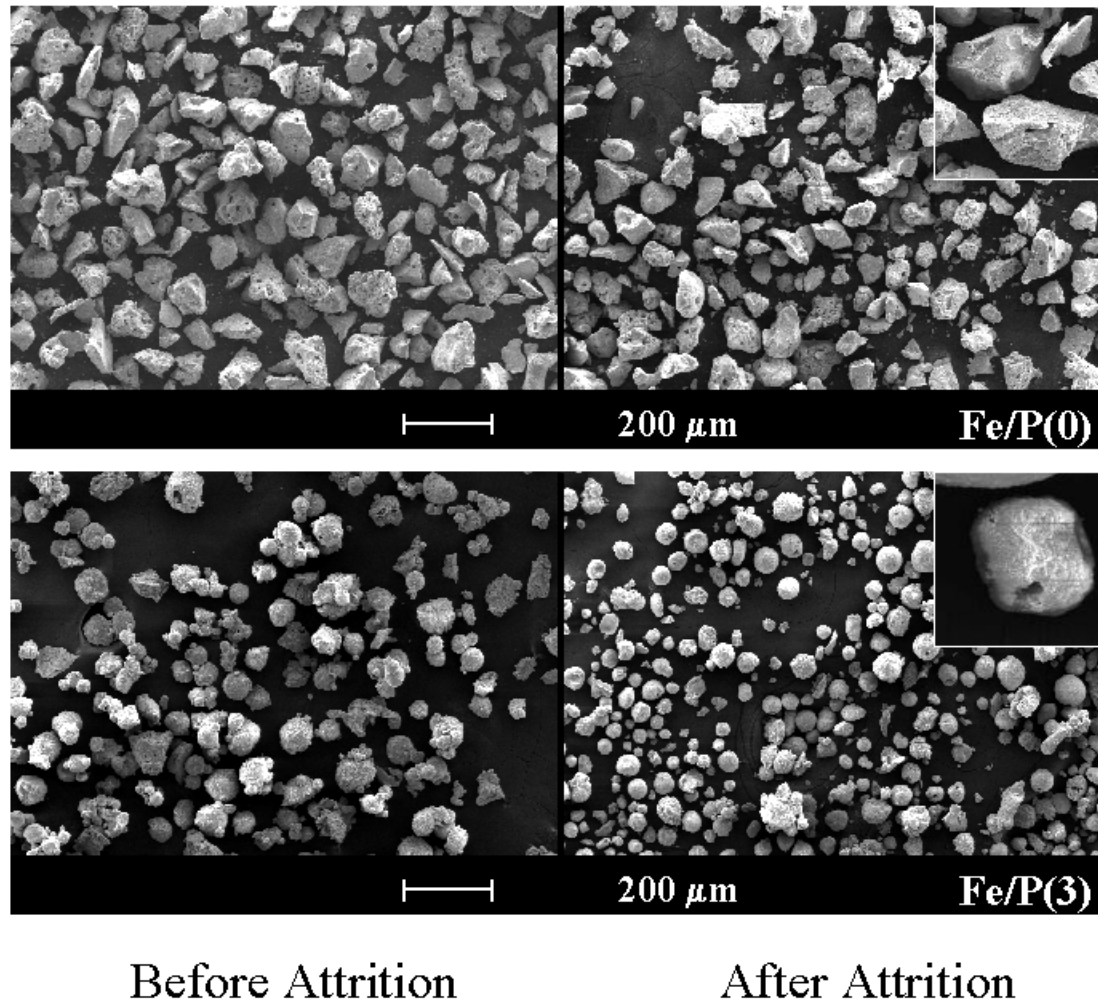
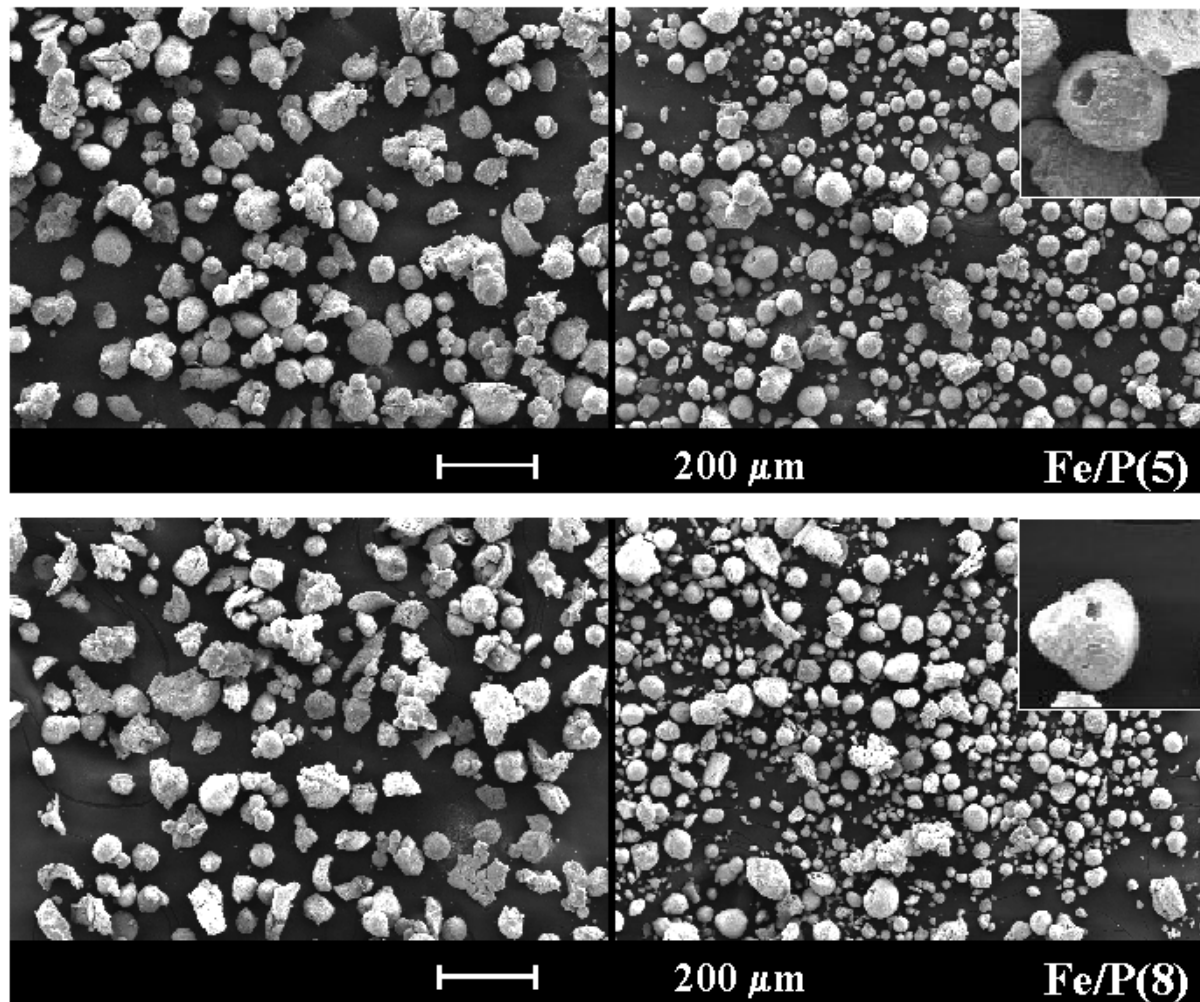


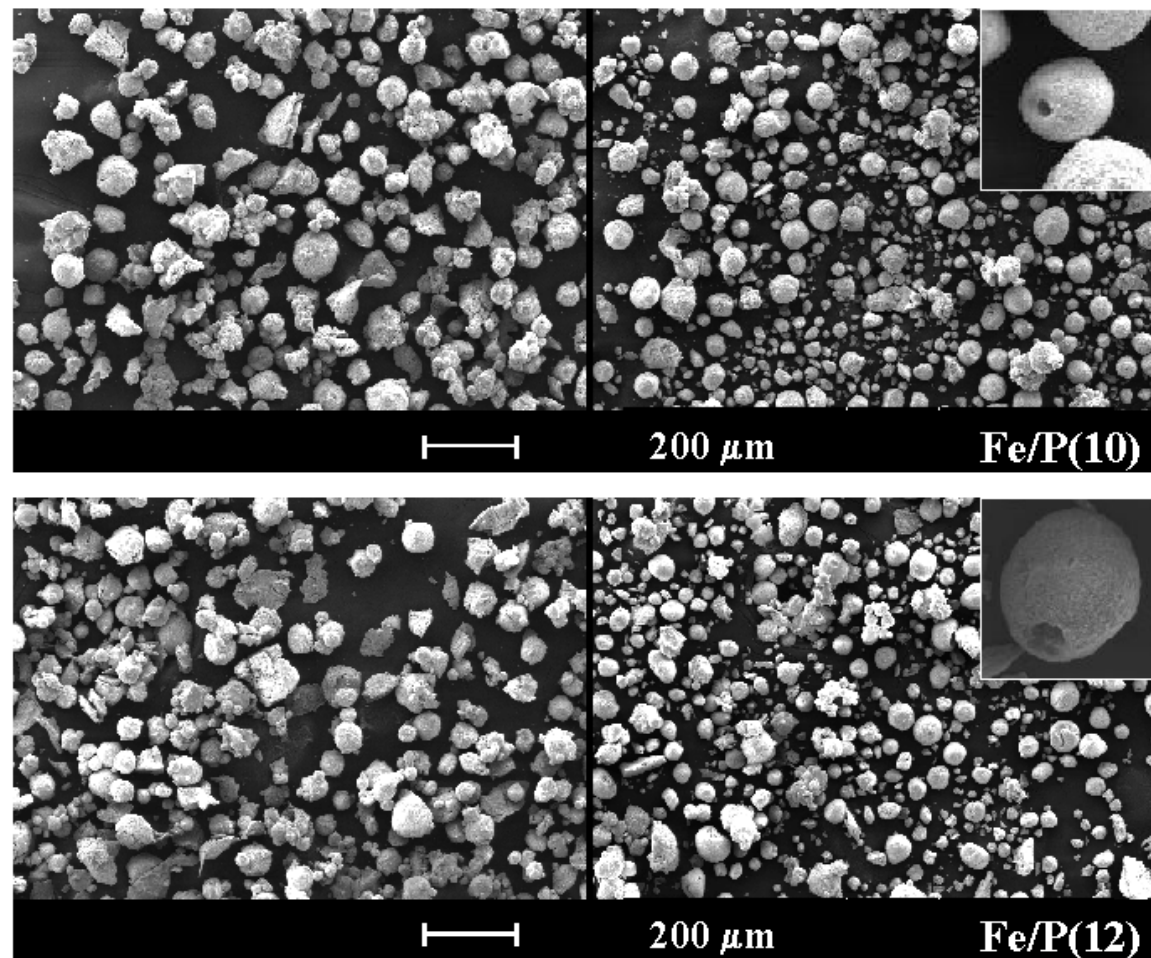
Figure 2a. SEM micrographs of Fe/P(0) and Fe/P(3) before and after attrition.



Before Attrition

After Attrition

2b. SEM micrographs of Fe/P(5) and Fe/P(8) before and after attrition.



Before Attrition

After Attrition

Figure 2c. SEM micrographs of Fe/P(10) and Fe/P(12) before and after attrition.

The precipitated SiO<sub>2</sub> network incorporated in the catalysts can be seen by SEM after acid leaching, which dissolves Fe, Fe oxide, Cu, and K and leaves mainly the SiO<sub>2</sub> structure. Catalyst particles were treated with 30% HCl solution (pH=1) for 48 hours to ensure that those elements were leached out. The residue was washed thoroughly with deionized water under vacuum filtration and dried under vacuum at room temperature to avoid agglomeration by heating. Figure 4 shows typical SiO<sub>2</sub> structures seen with and without interior holes. Both structures showed a smoother texture of SiO<sub>2</sub> surface at this magnification, which differs from the more porous SiO<sub>2</sub> structures seen in spray-dried Fe catalysts prepared earlier with either binder or binder + precipitated SiO<sub>2</sub>.<sup>27</sup> The SiO<sub>2</sub> structures obtained by leaching catalysts after attrition were identical, consistent with the fact that there was not a great deal of attrition and most was due to a break up of agglomerates (Figures 2A-C).

## 5.0 DISCUSSION

### 5.1 Catalyst Attrition Resistance

Although ‘weight percentage of fines lost’ and ‘net change in volume moment’ are both used as attrition indices, they have different physical meanings. While weight percentage of fines lost is a representative of the amount of fines generated and elutriated (ca. <22 μm), net change in volume moment represents a change of volume mean average particle size, weighted mostly towards the larger particles.<sup>60</sup> Therefore, a combination of these two attrition indices have been used in our attrition studies to help delineate physical attrition both by fracture (generating large broken particles) and abrasion/erosion (generating fines). Due to the difference in their physical meanings, it would not be surprising if the values of these two parameters were not identical with each other. However, for this spray-dried Fe catalyst series prepared with precipitated SiO<sub>2</sub> only, both attrition indices show similar trends in their relationship to the amount of precipitated SiO<sub>2</sub> added (Figure 1). These results suggest that the change in average particle size (mostly large particles) occurred in a similar degree as fines generated and possibly that the breakage of large particles facilitated the generating of fines. Weight percentage of fines lost is, however, considered the most important attrition index in our studies since fines generated cause the

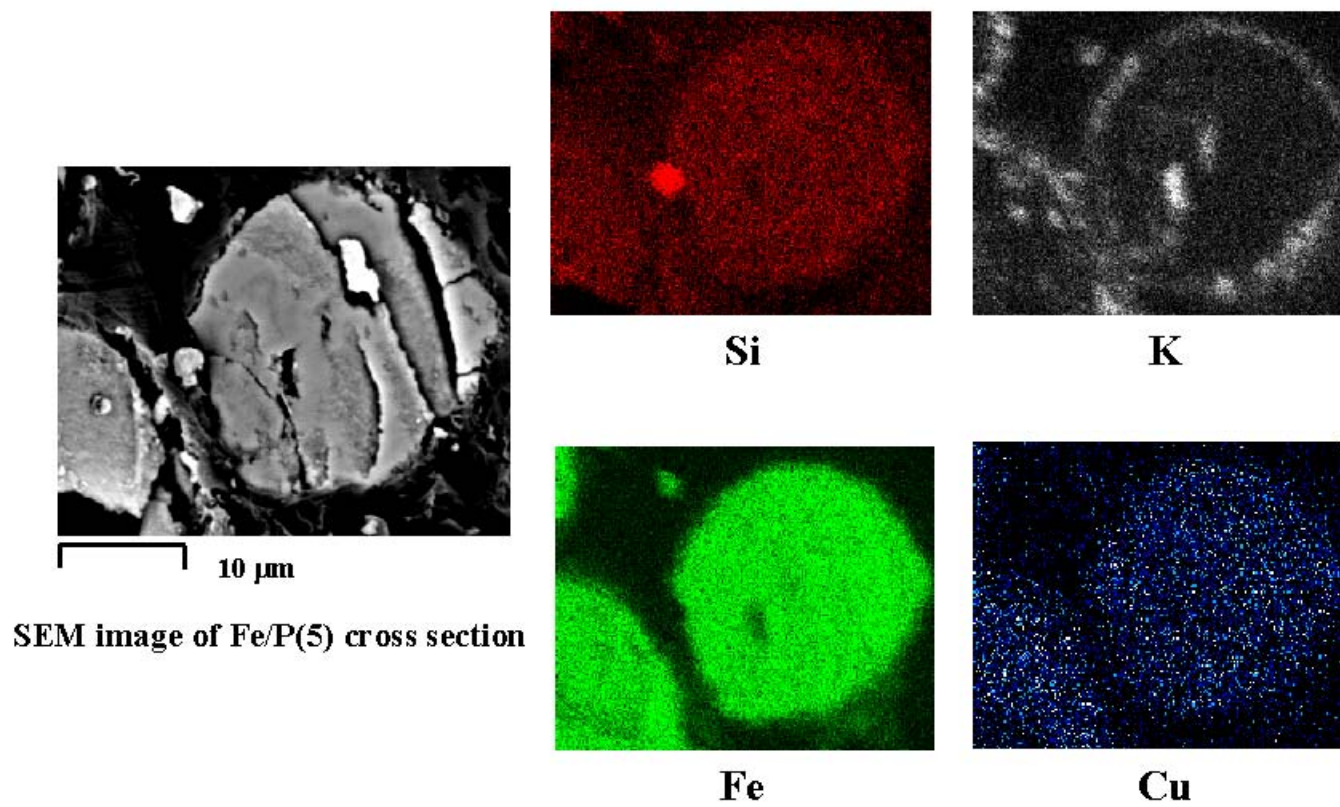


Figure 3. EDXS results for the cross section of a typical Fe/P(5) particle.



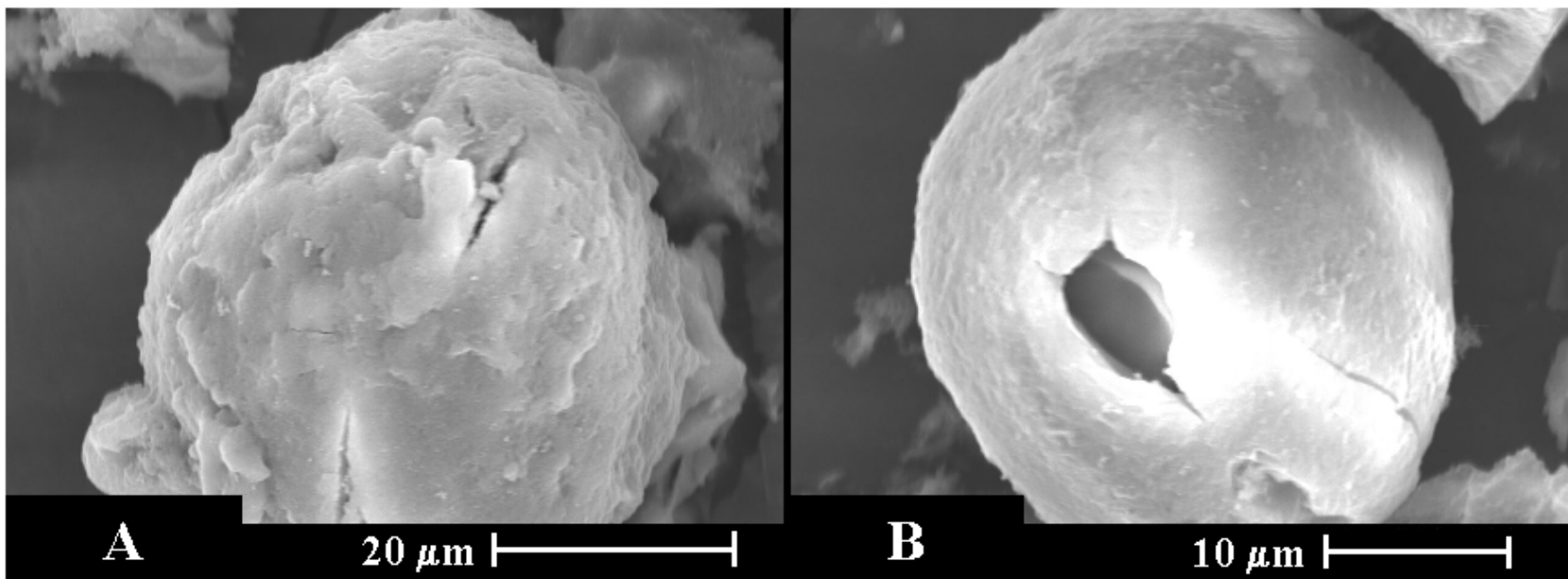


Figure 4. SEM micrographs of typical  $\text{SiO}_2$  structures after acid leaching [Fe/P(12)]: (A) typical structure, (B) particle with interior.

aforementioned problems in SBCR operation and since these catalysts were developed for SBCR usage.

In our previous study<sup>60</sup> to determine the effect of SiO<sub>2</sub> type (binder vs. precipitated + binder) and concentration on attrition resistance of spray-dried Fe catalysts, the catalyst having only binder SiO<sub>2</sub> (Fe/P(0)/B(11)) at the moderate concentration of ca. 11 wt% SiO<sub>2</sub> showed the highest attrition resistance (least attrition). Addition of precipitated SiO<sub>2</sub> to this composition (Fe/P(y)/B(10)) was found to reduce attrition resistance sharply. The use of precipitated silica alone at high loadings (20-25 wt%) is well known to result in poor attrition resistant Fe catalysts. However, the effect of having only precipitated SiO<sub>2</sub> at lower concentrations, especially in spray-dried Fe catalysts, was not determined. Thus, it is useful to compare the attrition results of the catalysts in this study (which had the same Fe/Cu/K ratios as those previously studied but were prepared with only precipitated SiO<sub>2</sub>) with those from the previous study<sup>60</sup> (see Figure 5). Catalysts with only precipitated SiO<sub>2</sub> at concentrations <12 wt% showed significantly improved attrition resistance than other catalyst compositions. At a moderate total SiO<sub>2</sub> concentration about 11 wt%, the curves for the three catalyst series essentially intersect, indicating that some particle property of these spray-dried iron catalysts prepared with similar amounts but different types of SiO<sub>2</sub> could possibly have an influence on their attrition resistances.

The two catalysts having the lowest concentrations of binder SiO<sub>2</sub> seem to have had somewhat different attrition properties than the rest of the catalysts (Figure 5). This was possibly due to their being prepared at different solution pH and/or drying temperature, which may have caused lower particle densities than otherwise expected. This effect has been shown to be reproducible.

In the earlier studies,<sup>60,63</sup> we found that catalyst attrition depended greatly on catalyst particle density and that this was not due to a bias in the attrition test. Figure 6 shows % fines lost versus particle density for catalysts prepared with only precipitated SiO<sub>2</sub> and for catalysts prepared with only binder SiO<sub>2</sub> or with binder + precipitated SiO<sub>2</sub>.<sup>2</sup> The results for the catalysts having only precipitated SiO<sub>2</sub> are completely consistent with the previous data and therefore confirm the strong relationship between these two parameters. Thus a catalyst with a high particle density exhibits low attrition or, in other words, has high attrition resistance. On the other hand, too dense catalysts, however, may not be fluidized well enough to obtain a good dispersion in a reactor slurry, leading to poor contact between reactants and catalyst particles.

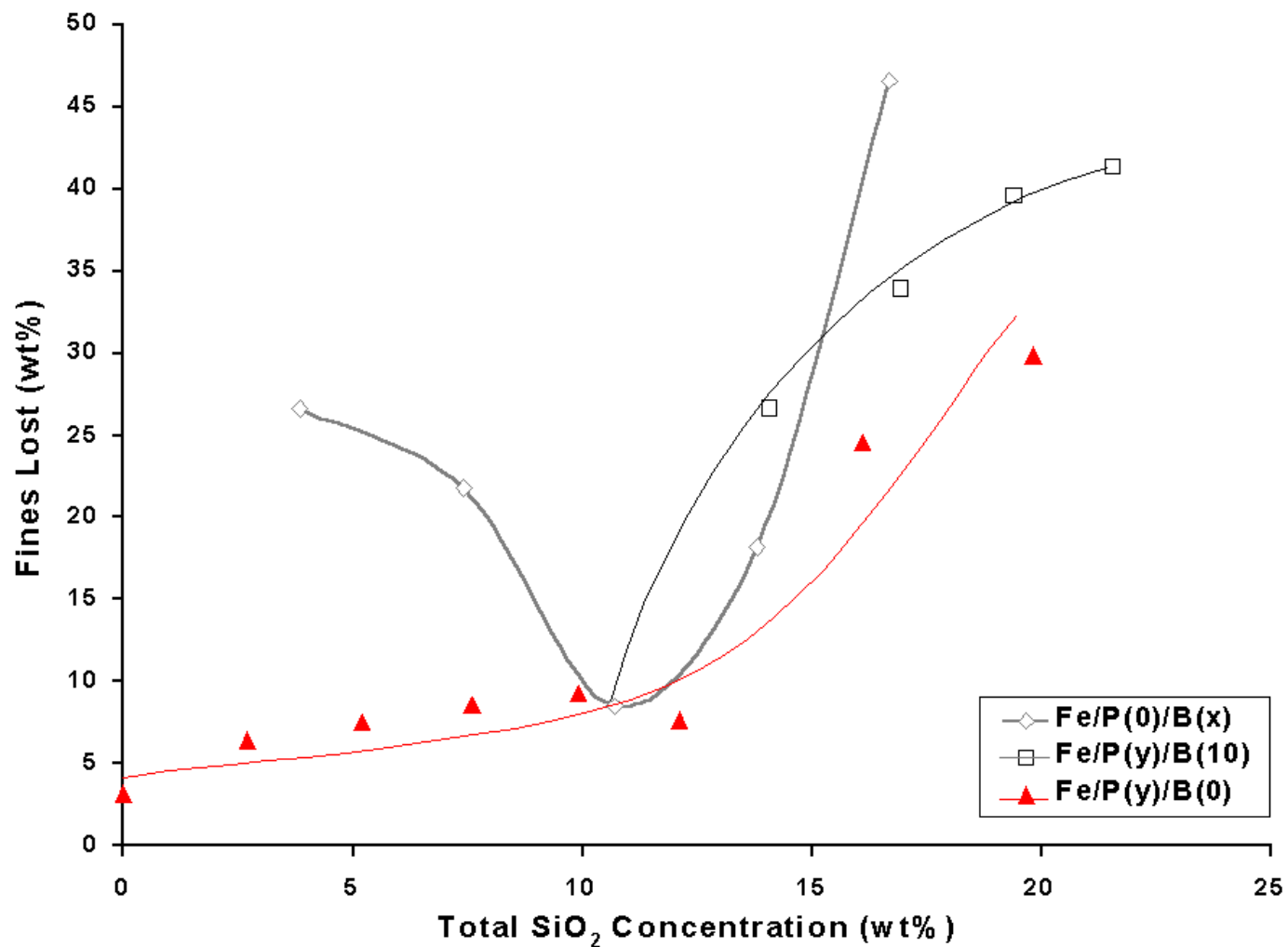


Figure 5. Weight percentage of fines lost vs. total concentration of SiO<sub>2</sub> for different series of spray-dried Fe FT catalysts: B refers to binder SiO<sub>2</sub>; P refers to precipitated SiO<sub>2</sub>; x and y refer to the amount of binder and precipitated SiO<sub>2</sub> added, respectively. [Data for Fe/P(0)/B(x) and Fe/P(y)/B(10) from ref. 1].

Thus, attrition resistance is not only the important factor in catalyst design for SBCR usage. High surface area and proper particle density are also needed to obtain high catalytic activity and good fluidization, respectively. The presence of SiO<sub>2</sub> in Fe FT catalysts enhances their active surface areas but lowers the density of the catalyst as well as their attrition resistances. Therefore, the amount of SiO<sub>2</sub> added must be optimized to obtain high catalytic activity, high attrition resistance, and good fluidization of catalyst particles when used in SBCRs.

## 5.2 SiO<sub>2</sub> Structure

After acid leaching, precipitated SiO<sub>2</sub> particles (Figure 4) were not found significantly changed in either size or shape from the original catalyst particles. Moreover, those particles with interior-hole structures maintained the same structure (with holes) after being acid leached. All these observed structures after acid leaching as well as the EDXS results suggest that the structure of precipitated SiO<sub>2</sub> in the catalyst particles was a continuously network (skeleton). There is no evidence that suggests the SiO<sub>2</sub> existed as discrete, non-continuous parts in the original catalyst particles that somehow agglomerated during acid leaching. Although some SiO<sub>2</sub> particles were found to have interior holes, in no way did they have an 'egg shell' structure. Precipitated SiO<sub>2</sub> was evenly distributed, as shown by EDXS (Figure 3), throughout the particles, similarly to Fe.

The surface morphology of the acid leached precipitated SiO<sub>2</sub> particles (Figure 4) both with and without interior holes was relatively more smooth compared to the porous SiO<sub>2</sub> structures resulting from acid leaching of the catalysts prepared with binder SiO<sub>2</sub> or binder + precipitated SiO<sub>2</sub>.<sup>2</sup> However, the difference in this morphology did not seem to be a major factor for the physical strength of the catalysts (Figure 5).

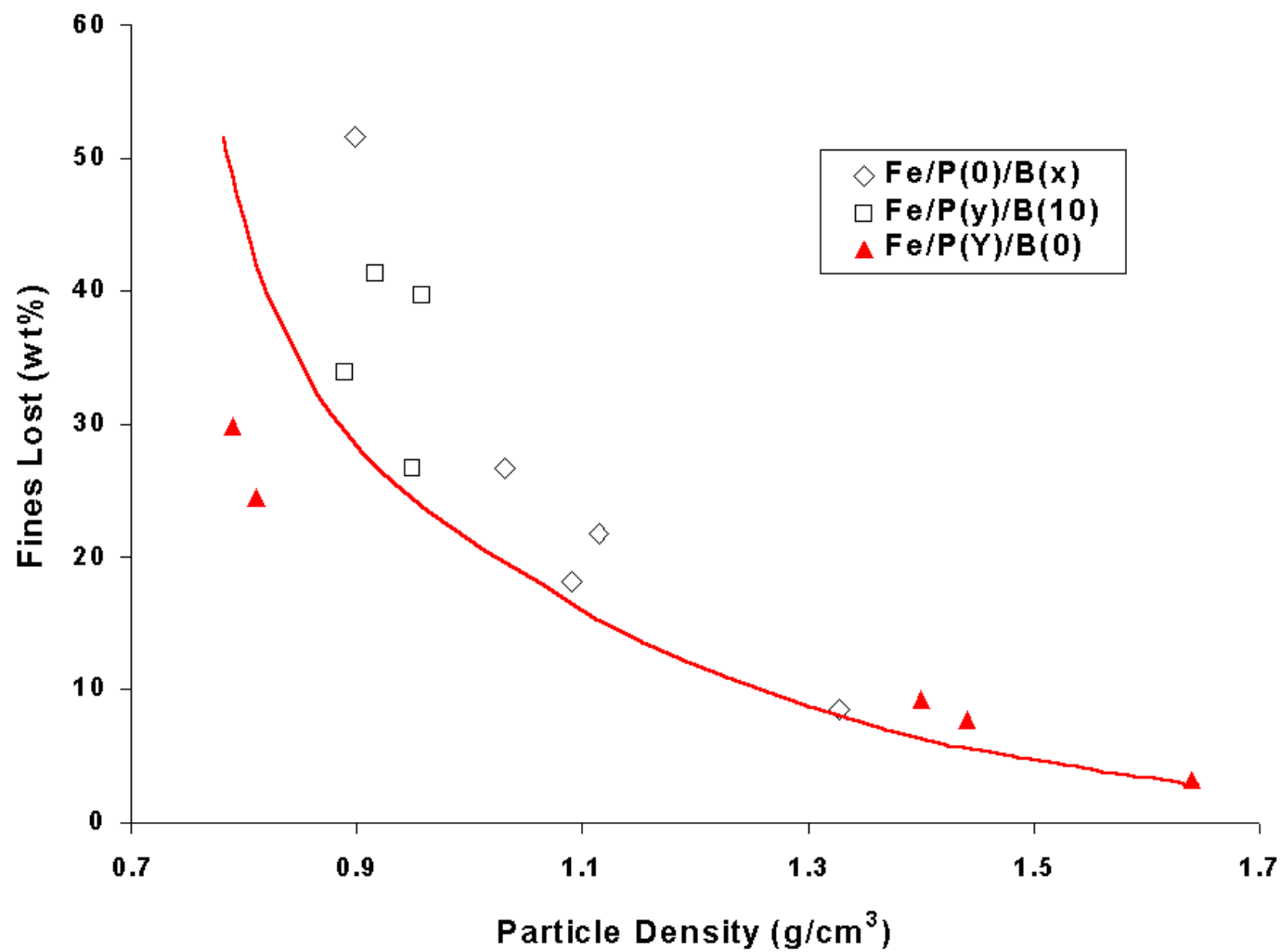


Figure 6. Weight percentage of fines lost vs. average particle density of calcined Fe/P(y), Fe/B(x), and FE/P(y)/B(10) catalysts.

### 5.3 Slurry Reactor Tests

Two catalysts were used in the present study and their compositions are: 100 Fe/5 Cu/4.2 K/1.1 (B) SiO<sub>2</sub> (designated as Catalyst B, since it contains binder silica) and 100 Fe/5 Cu/4.2 K/11 (P) SiO<sub>2</sub> (Catalyst P, containing precipitated silica). Compositions are given in parts by weight, except for the silica content, which represents weight percent of silica in the fresh catalyst (based on total catalyst weight).

The reactor testing was conducted at Texas A & M University. Details of the reactors tests such as experimental set up, operating procedures and product quantification can be found elsewhere. A brief description of experimental apparatus is summarized here. Experiments were conducted in a 1-dm<sup>3</sup> stirred tank reactor (autoclave Engineers, Erie, Pennsylvania). A standard six-blade turbine impeller of 3.2 cm in diameter and a stirrer speed of 1200 rpm were used in all experiments. The feed gas flow rate was adjusted with a mass flow controller and passed through a series of oxygen removal, alumina and activated charcoal traps to remove trace impurities. After leaving the reactor, the exit gas passed through a series of high and low (ambient) pressure traps to condense liquid products. High molecular weight hydrocarbons (wax), withdrawn from the slurry reactor through a porous cylindrical sintered metal filter, and liquid products, collected in the high and low pressure traps, were analyzed by gas chromatography. The reactor was charged with ~15 g of as-received catalyst dispersed in approximately 400 g of Durasyn-164 oil (hydrogenated 1-decene homopolymer). Slurry samples were withdrawn from the reactor at TOS = 0 hours (TOS = time on stream) and at the end of the test. Durasyn-164 oil (or hydrocarbon wax produced during F-T synthesis) was removed by filtration aided by addition of a commercial solvent Varsol 18 (a mixture of liquid aliphatic and aromatic hydrocarbons).

Catalysts were reduced *in situ* with CO at 280°C, 0.8 MPa, 3 NL/(g-cat·h) (where NL/h denoted volumetric gas flow rate at 0°C and 1 bar) for 12 hours. After the pretreatment, the catalysts were initially tested at 260°C, 2.1 MPa, H<sub>2</sub>/CO = 2/3, and gas space velocity of either 3.5 NL/(g-Fe·h) or 3.5 NL/(g-Fe·h).

#### 5.4 Catalyst Activities and Selectivity in STSR Tests

Results from tests precipitated catalyst and binder catalyst are shown in Figures 7-14. The catalysts were pretreated under the same conditions, and the process conditions were similar in both tests except for a 110 h time period (224-334 h) in run for precipitated when a significantly higher gas space velocity was employed.

In both tests, during the first 50-80 h on stream, the syngas conversion increased with time reaching 85-87%. After reaching the maximum conversion, the catalysts started to deactivate and at 200 h on stream the syngas conversion was about 76% in both tests. During the first 200 h of testing, the syngas conversion values were about the same in both tests. Since the gas space velocity in run for binder was lower than that used in precipitated (3.1 vs. 3.5 NL/g-Fe · h), we conclude that the intrinsic activity of precipitated catalyst is higher than that of binder catalyst.

In run for precipitated catalyst, the gas space velocity was increased to 5.2 NL/g-Fe · h at 224 h on stream, which was accompanied by decrease in conversion and further catalyst deactivation between 225 and 280 hours on stream. Between 280 and 334 hours, the conversion was fairly stable (43-44%). After returning to the baseline conditions at 335 h, the syngas conversions were about 60%, but the activity continued to decrease with time and at the end of the run (384 h) the conversions were about 48%. The average loss in syngas conversion (catalyst deactivation rate) between 80 and 224 hours was 0.09%/hour, whereas the average conversion loss for the time period between 80 and 384 hours was 0.145%/hour (3.84%/day). This shows that catalyst deactivation was faster during the latter portion of the test.

In run for binder catalyst, the process condition was constant. After 204 h on stream, the syngas conversion decreased abruptly from 78% to 66%, and remained at this lower value during the next 40 hours of testing. This drop in conversion was probably caused by reduction in stirring rate, due to malfunctioning of an electric motor. At 247 h the test was suspended due to complete stoppage of the stirrer. During the test interruption, the catalyst was kept in N<sub>2</sub> atmosphere at 120°C for 30 days. After the test was resumed, the initial conversion was similar to that observed at 204 h, i.e., before the problem with the electric motor arose. However, the catalyst activity continued to decrease with time reaching 60% at the end of the test (449 h). The average rate of catalyst activity loss between 53 and 449 h was 0.0676%/hour (1.62%/day), which is significantly smaller than that observed in the precipitated catalyst situation.

Both catalysts exhibited very high WGS activity. Selectivity to CO<sub>2</sub> increased quickly with time reaching a stable value of about 49% (not shown). The WGS activity remained stable throughout the test, even though the F-T activity decreased with time.

Hydrocarbon selectivities (CH<sub>4</sub> and C<sub>5+</sub>) were similar in both tests. Methane selectivity (carbon atom basis) decreased during the first 150 h of testing, reaching a fairly stable value of 2.0 ± 0.2%. Methane selectivity was not markedly affected by changes in conversion and/or process conditions. Selectivity of C<sub>5+</sub> hydrocarbons (liquids and wax) was high in both tests. It increased to 84-86% during the first 130-150 hours of testing and then decreased somewhat after about 200 h on stream. Liquid plus wax selectivity (fraction of C<sub>5+</sub> hydrocarbons among total hydrocarbons on carbon atom basis) was also not markedly affected by changes in conversion level and/or process conditions.

## **6.0 Conclusion**

Spray-dried catalysts with compositions 100 Fe/5 Cu/4.2 K/11 (P) SiO<sub>2</sub> and 100 Fe/5 Cu/4.2 K/1.1 (B) SiO<sub>2</sub> investigated in STSR have excellent selectivity characteristics (low methane and high C<sub>5+</sub> yields), but their productivity and stability (deactivation rate) needs to be improved. Mechanical integrity (attrition strength) of these two catalysts was markedly dependent upon their morphological features. The attrition strength of the catalyst made out of largely spherical particles (1.1 (B) SiO<sub>2</sub>) was considerably higher than that of the catalyst consisting of irregularly shaped particles (11 (P) SiO<sub>2</sub>). Improvements in spray drying operating parameters resulting in narrower PSD and higher sphericity could lead to further improvements in the attrition strength.



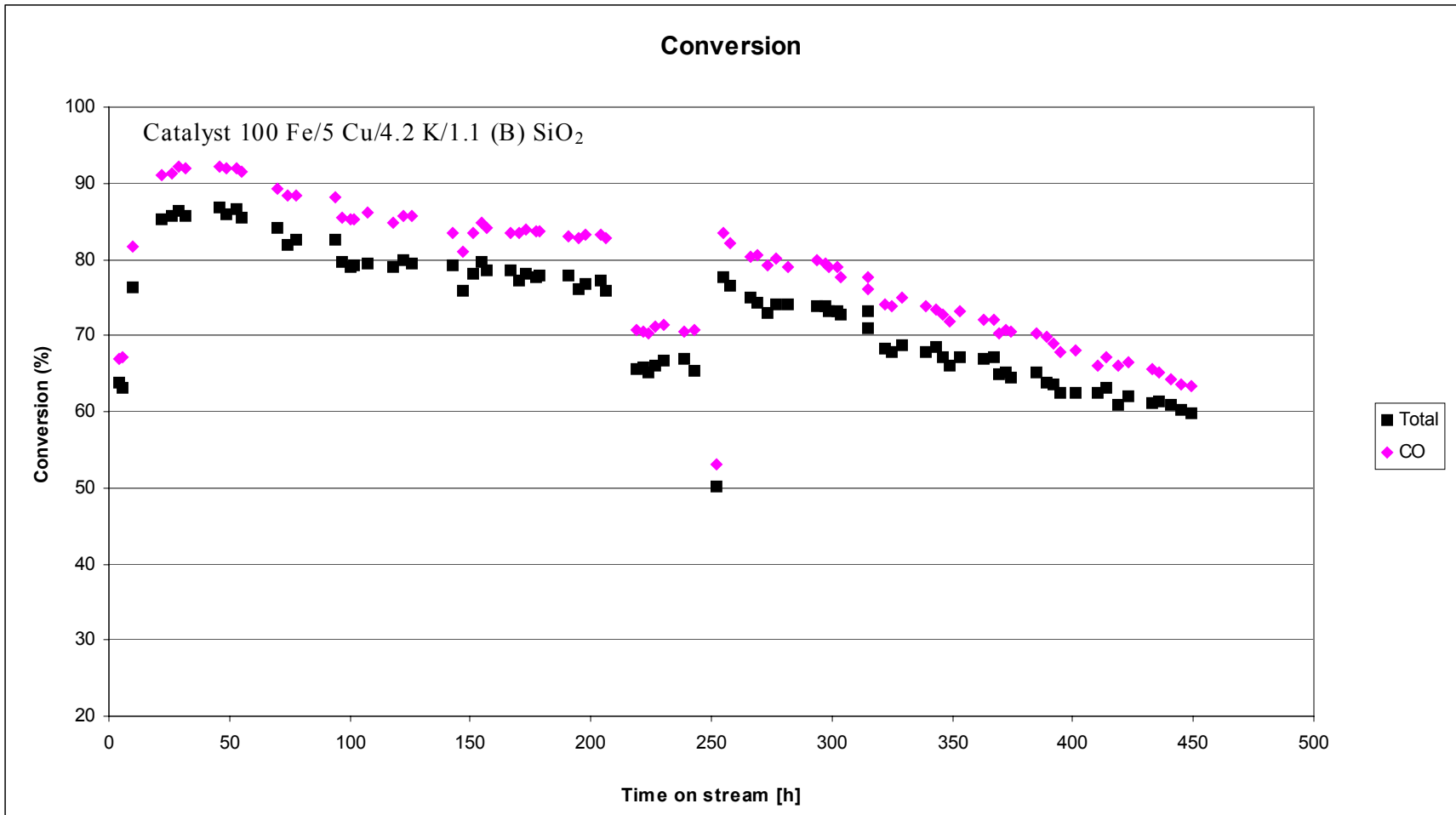


Figure 7. Syngas Conversion with Time On-Stream for Binder Silica

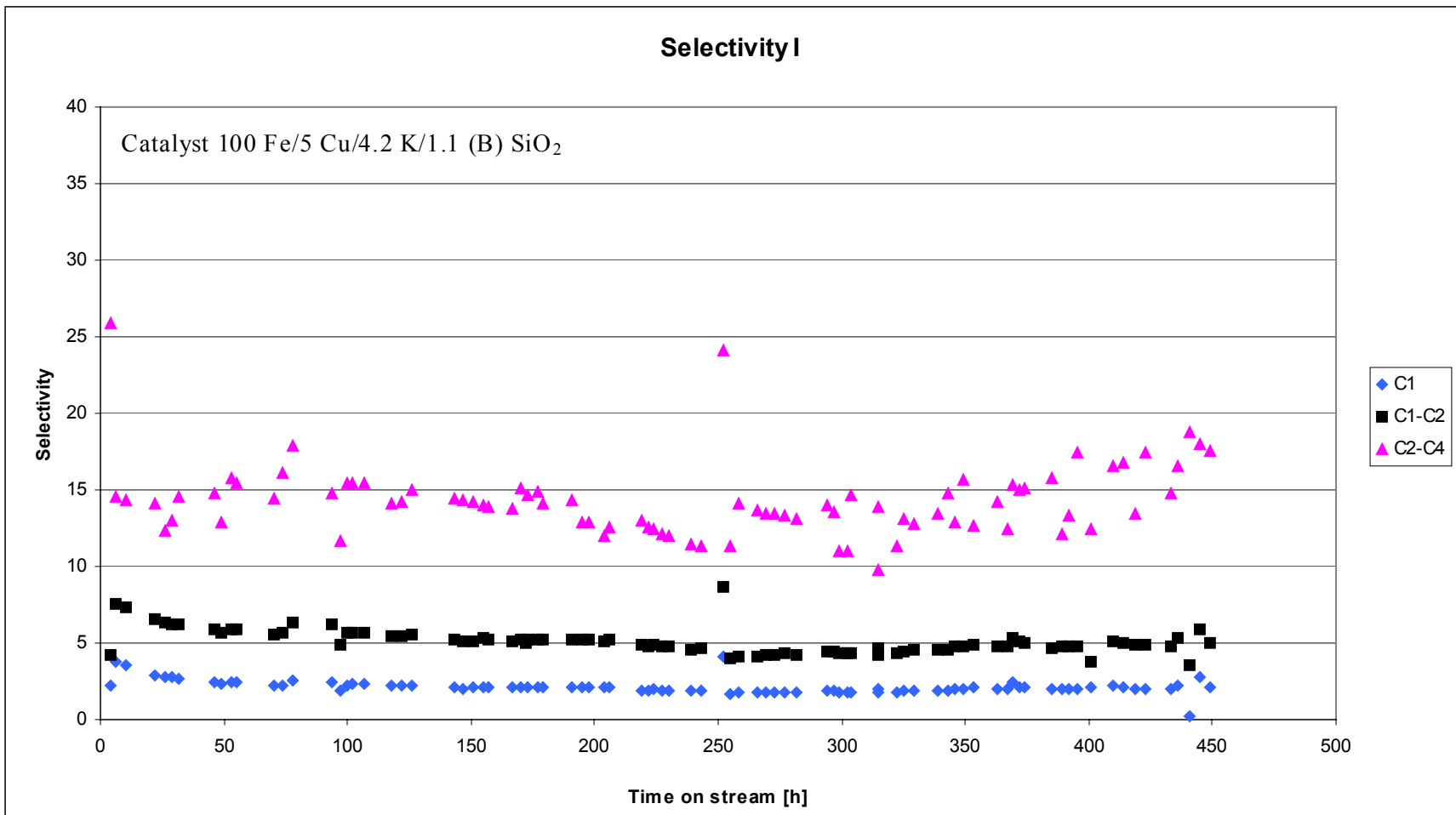


Figure 8. C<sub>1</sub>-C<sub>4</sub> Selectivity with Time on stream for Binder Silica.

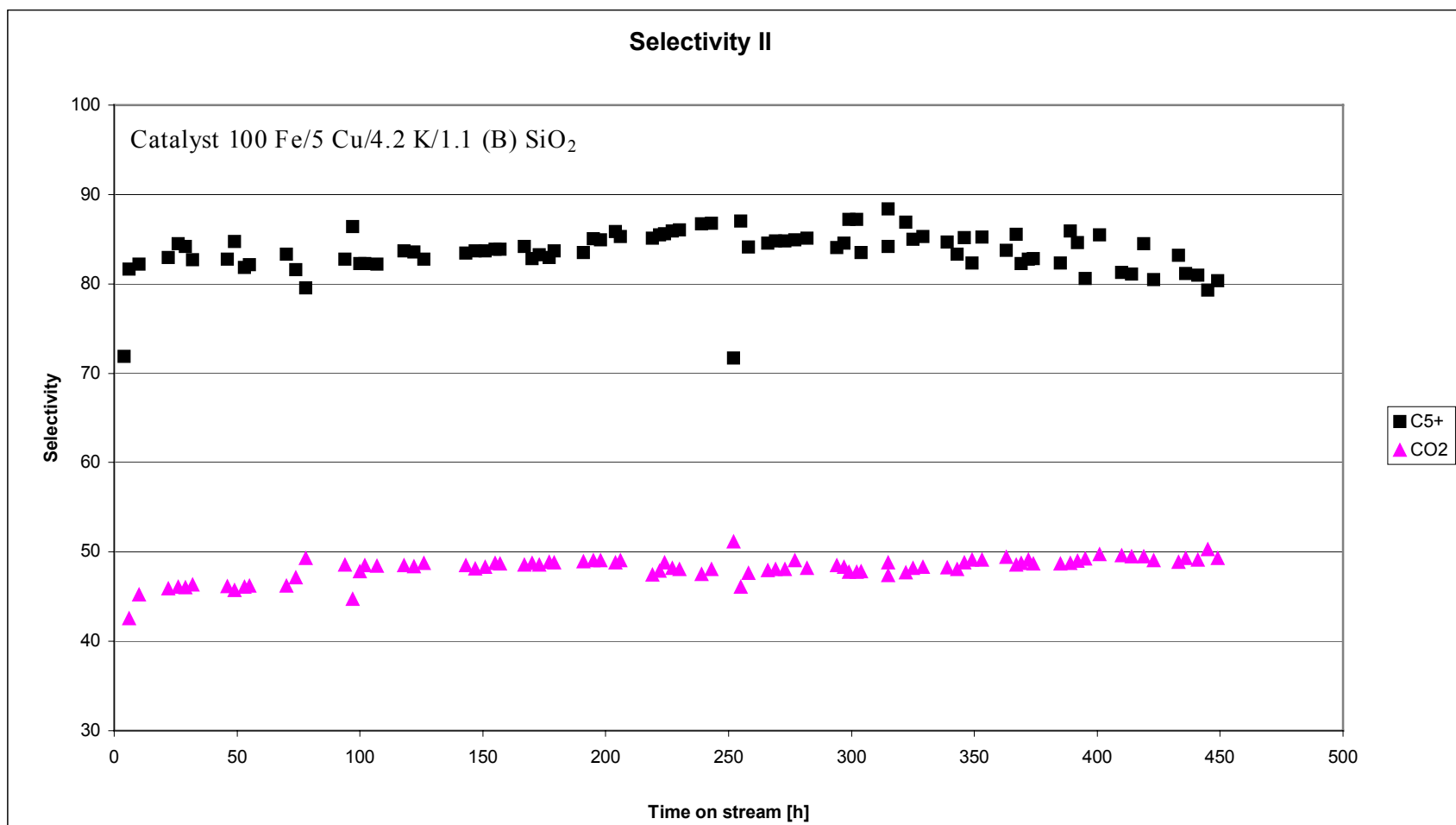


Figure 9. C<sub>5</sub>+ Selectivity with Time on Stream for Binder Silica.

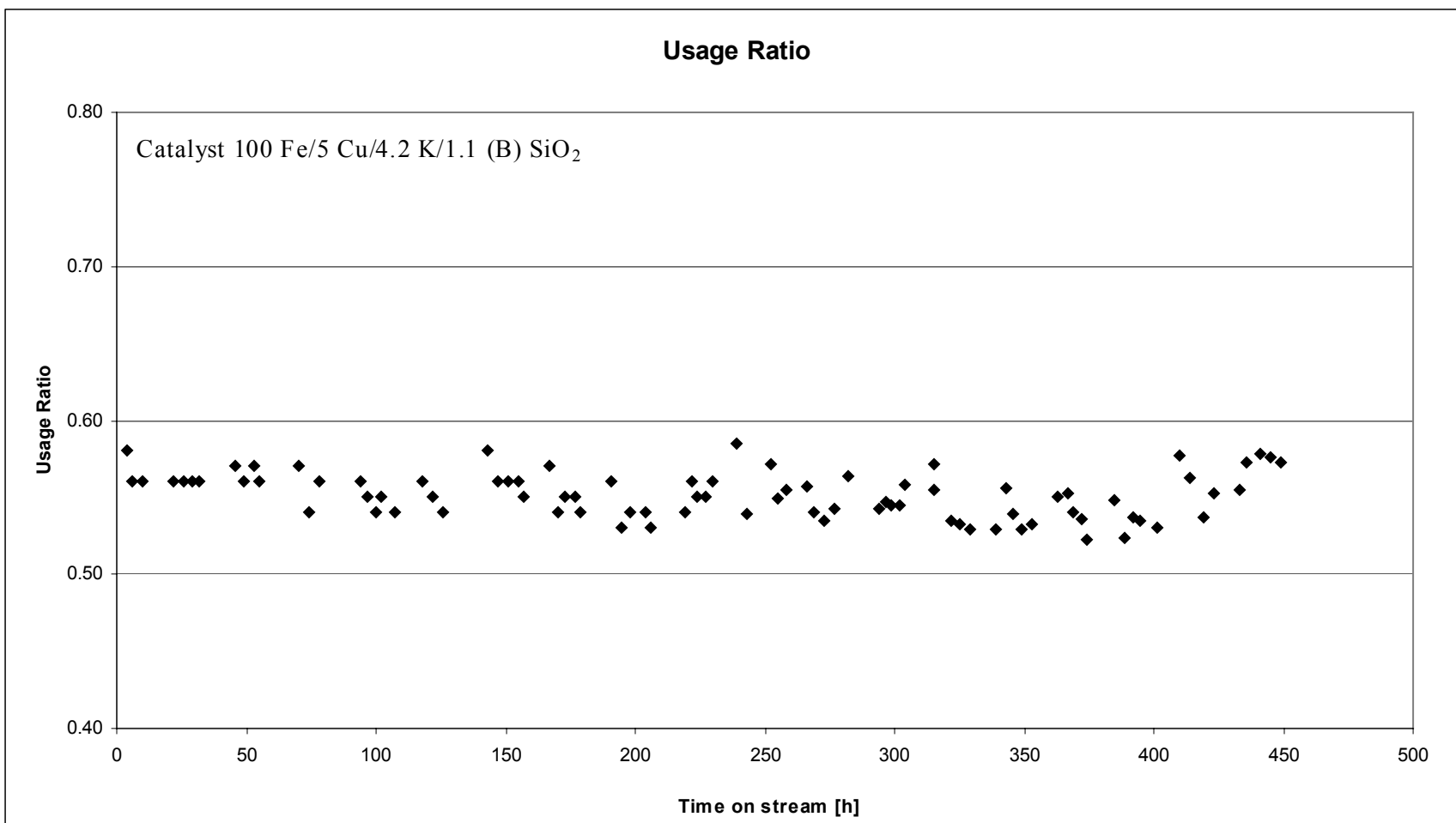


Figure 10. Usage Ratio with Time on Stream for Binder Silica.

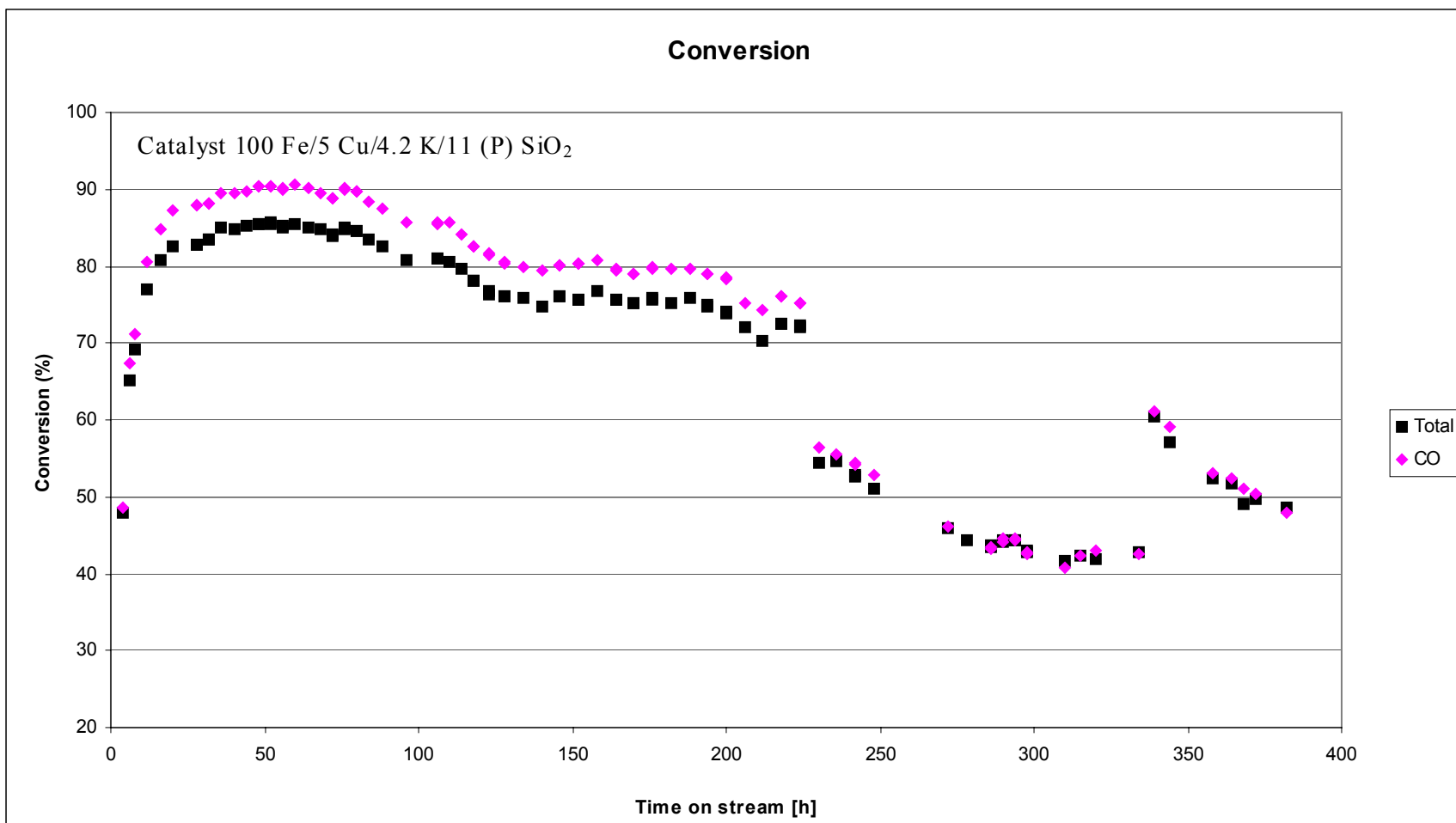


Figure 11. Syngas Conversion with Time On-Stream for Binder Silica.

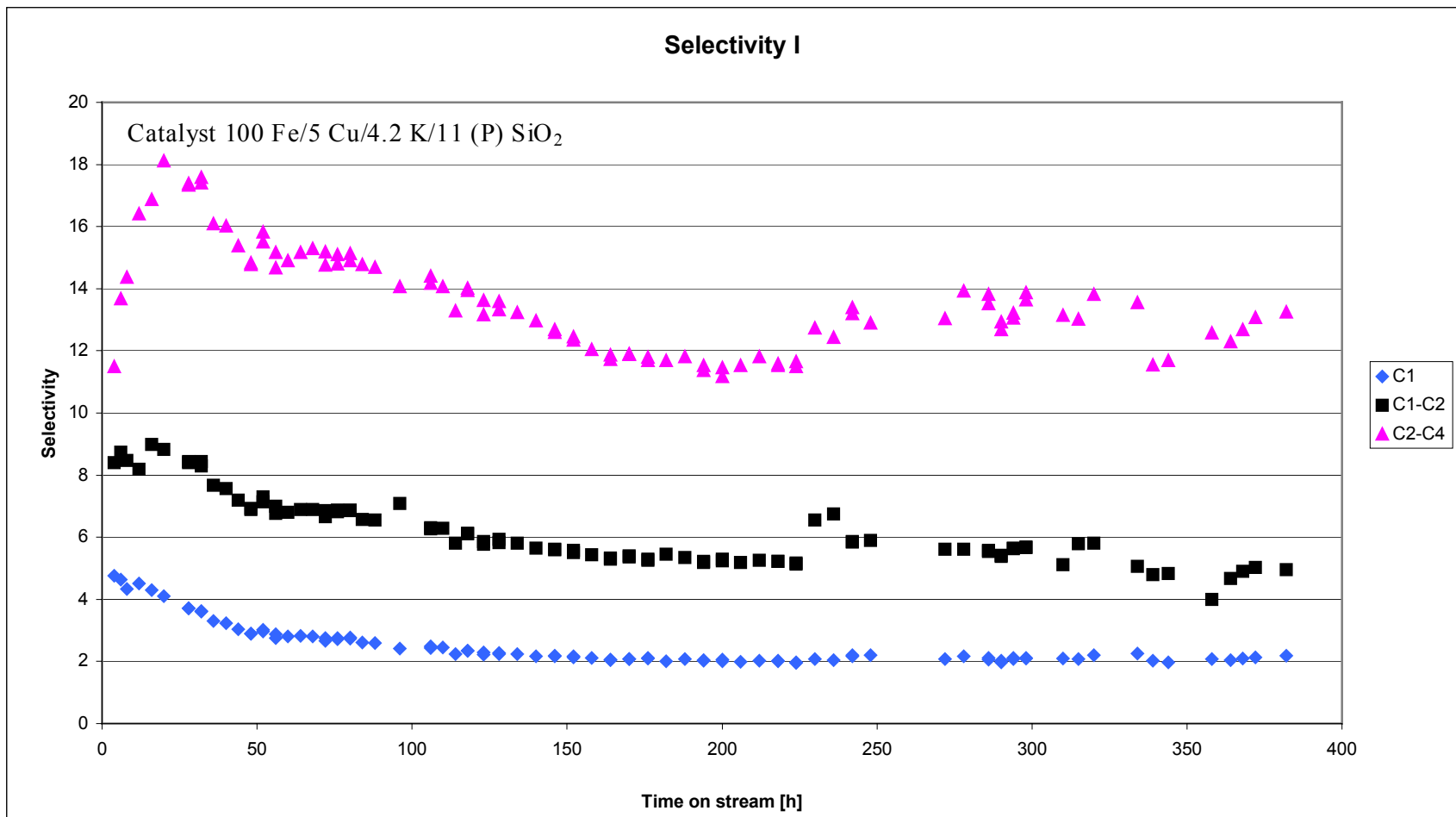


Figure 12. C<sub>1</sub>-C<sub>4</sub> Selectivity with Time On-Stream for Precipitated Silica.

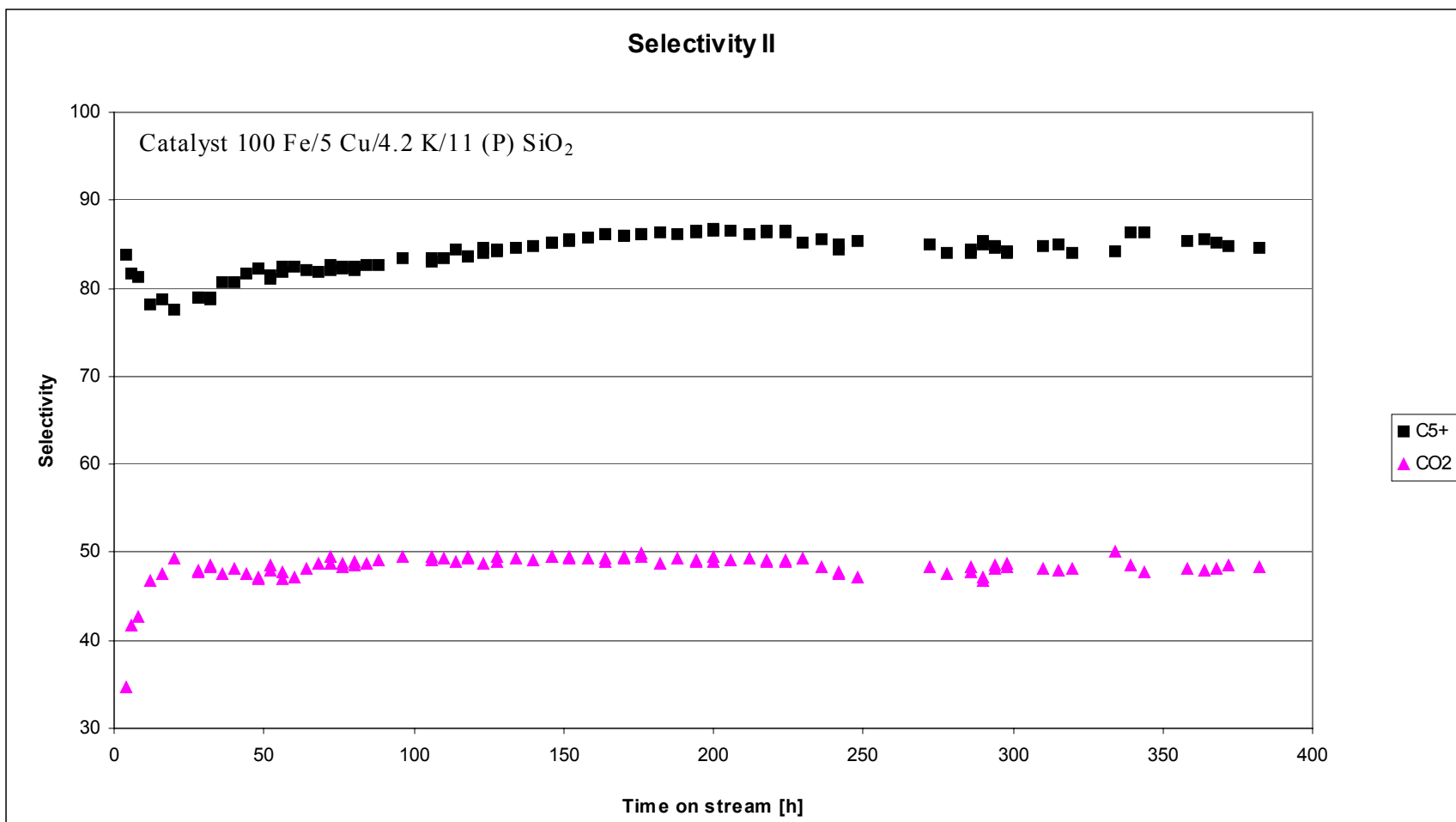


Figure 13. C<sub>5</sub>+ Selectivity with Time On-Stream for Precipitated Silica.

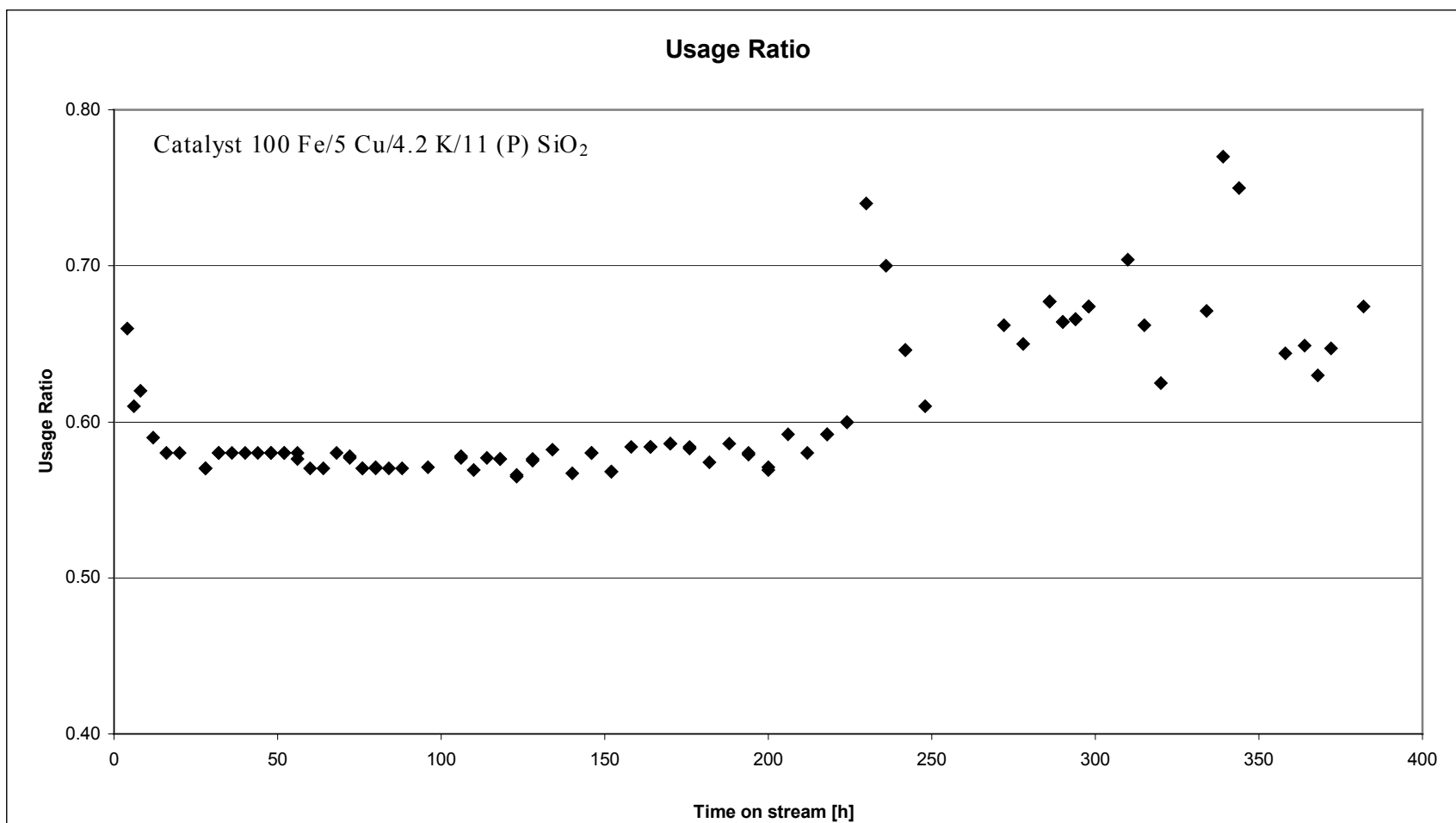


Figure 14. Usage Ratio with Time On-Stream for Precipitated Silica.



## Literature References

1. Allen, T., *Particle Size Measurement*, 5<sup>th</sup> ed., Chapman & Hall, New York (1997).
2. Amelse, J.A. butt, J.B., and Schwartz, L.H., *J. Phys. Chem.*, 82, 558(1978).
3. Amelse, J.A., Schwartz, S.T., and Butt, J.B., *J. Catal.*, 87, 179(1984).
4. Anderson, R.B., *The Fischer-Tropsch Synthesis*; Academic Press: Orlando, FL, 1984.
5. ASTM D-32.02.06, DI Test of Attrition Resistance.
6. Bessel, S., U.S. Patent, 5, 126, 377(1992).
7. Bhatt, B.L., Schaub, E.S., Hedorn, D.C., Herron, D.M., Studer, D.W., Brown, D.M., in "Proc. Of Liquefaction Contractors Review Conference", (G.J. Stiegel and R.D. Srivastava, Eds.), U.S. Department of Energy, Pittsburgh, 1992, p. 403.
8. Bukur, D.B., and Lang, X., *Studies in Surface Science and Catalysis*, 119, 118 (1998).
9. Bukur, D.B., Carreto-Vazquez, V., Pham, H.N., Datye, A.K. (submitted).
10. Bukur, D.B., Lang, X., *Ind. Eng. Chem. Res.* 38 (1999) 3270.
11. Bukur, D.B., Lang, X., Mukesh, D., Zimmerman, W.H., and Li, C., *J. Catal.*, 29, 1588(1990b).
12. Bukur, D.B., Mukesh, D., and Patel, S.A., *Ind. Eng. Chem. Res.*, 29, 194 (1990a).
13. Bukur, D.B., Nowicki, L., Lang, X., *Chem. Eng. Sci.* 49 (1994) 4615.
14. Bukur, D.B., Nowicki, L., Manne, R.K., and Lang, X., *J. Catal.*, 155, 366(1995b).
15. Bukur, D.B., Okabe, K., Li, C., Wang, D., Rao, K.R.P.M., and Huffman, G.P., *J. Catal.*, 155, 353(1995a).
16. Bukur, D.B., Patel, S., and Lang, X., *App. Catal. A* 61 (1990) 329.
17. Butt, J.B., *Catal. Lett.*, 7, 61(1990).
18. Datye, A.K., and Shroff, M.D., Harrington, M.S., Sault, A.G., and Jackson, N.B., *Studies in Surface Science and Catalysis*, 107, 169 (1997).
19. Davis, B.H., Zu, L., and Bao, S., *Studies in Surface Science and Catalysis*, 107, 175 (1997).
20. Donnelly, T.J., and Satterfield, C.N., *Appl. Catal.*, 56, 231(1989).

21. Dry, Appl. Catal., 138, 319(1996).
22. Dry, M., in Catalysis: Science and Technology, Vol. 1, ed. By Anderson, J.R., Springer-Verlag, NY, 1981.
23. Gormley, R.J., Zaroachak, M.F., and Deffenbaugh, P.W., Appl. Catal. A: General, 161, 263(1997).
24. Jaeger, B., *Studies in Surface Science and Catalysis*, 107, 219 (1997).
25. Jager, B., Espinoza, R., *Catal. Today*, 23 (1995) 17.
26. Jager, B., Van Berge, P., Steynberg, A.P., *Stud. Surf. Sci. Catal.* 136 (2001) 63.
27. Jothimurugesan, K., Goodwin Jr., J.G., Gangwal, S.K., Spivey, J.J., *Catal. Today* 58 (2000) 335.
28. Jothimurugesan, K., Spivey, J.J., Gangwal, S.K., and Goodwin, J.G., *Studies in Surface Science and Catalysis*, 119, 215 (1998).
29. Jothimurugesan, K., Spivey, J.J., Gangwal, S.K., and Goodwin, Jr., J.G., Development of Fe Fischer-Tropsch Catalysts for Slurry Bubble Column Reactors, ACS meeting, Anaheim, CA, March 21-25, 1999a. Abstract accepted.
30. Jothimurugesan, K., Spivey, J.J., Gangwal, S.K., and Goodwin, Jr., J.G., Development of Fe Fischer-Tropsch Catalysts with High Attrition Resistance, Activity, and Selectivity, Spring AIChE meeting, Houston, TX, March 14-18, 1999b. Abstract accepted.
31. Jothimurugesan, K., Spivey, J.J., Gangwal, S.K., and Goodwin, Jr., J.G., Attrition Resistant Iron-Based Fischer-Tropsch Catalysis, 16<sup>th</sup> Meeting of the North American Catalysis Society, Boston, MA, May 30-June 4, 1999c. Abstract accepted.
32. Jothimurugesan, K., Spivey, J.J., Gangwal, S.K., Goodwin Jr., J.G., *Stud. Surf. Sci. Catal.* 119 (1998) 215.
33. Kalakkad, D.S., Shroff, M.D., Kohler, S., Jackson, N., Datye, A.K., *Appl. Catal. A* 133 (1995) 335.
34. Kalakkad, D.S., Shroff, M.D., Kohlers, S., Jackson, N., and Datye, A.K., *Appl. Catal.*, 133, 335 (1995).
35. Kolbel, H., and Ralek, M., *Catal. Rev.-Sci. Eng.*, 21, 225(1980).
36. Lang, X., Akgerman, A., and Bukur, D.B., *Ind. Eng. Chem. Res.*, 34, 73(1995).
37. Lee, S.K., Jiang, X., Keener, T.C., and Khang, S.J., *Ind. Eng. Chem. Res.*, 32, 2758 (1993).

38. Milburn, D.R., Komandur, V.R., Chary, V.R., O'Brien, R.J., and Davis, B.H., *Appl. Catal.*, 144, 133 (1996).
39. O'Brien, R.J., Raje, A., Keogh, R.A., Spicer, R.L., Xu, L., Bao, S., Srinivasan, R., Houpt, D.J., Chokkram, S., and Davis, B.H., Coal Liquefaction and Gas Conversion Contractors' Review Conference, 1995.
40. O'Brien, R.J., Xu, L., Bao, S., Raje, A., Davis, B.H., *Appl. Catal. A* 196 (2000) 173.
41. Pennline, H.W., Zaroachak, M.F., Stencel, J.M., and Diehl, J.R., *Ind. Eng. Chem. Res.*, 26, 595 (1987).
42. Pham, H.N., Datye, A.K., *Catal. Today* 58 (2000) 233.
43. Pham, H.N., Nowicki, L., Xu, J., Datye, A.K., Bukur, D.B., C. Bartholomew, *Ind. Eng. Chem. Res.* (in press).
44. Pham, H.N., Reardon, J., Datye, A.K., *Powder Technol.* 103 (1999) 95.
45. Pham, H.N., Viergutz, A., Gormley, R.J., Datye, A.K., *Powder Technol.* 110 (2000) 196.
46. Rao, V.U.S., Stiegel, G.J., Cinquegrane, G.J., and Srivastava, R.D., *Fuel Proc. Technology*, 30, 83 (1992).
47. *Satterfield, Heterogeneous Catalysis in Practice, 1991.*
48. Sault, A.G., and Datye, A.K., *J. Catal.*, 140, 136(1993).
49. Shroff, M.D., Kalakkad, D.s., Coulter, K.E., Sault, A.G., and Datye, A.K., *J. Catal.*, 156, 185 (1995).
50. Singleton and Regier, *Hydrocarbon Processing*, 62, 71 (1983).
51. Soled, G., Iglesia, E., and Fiato, R.A., *Catal. Lett.*, 7, 271 (1990).
52. Srinivasan, R., Xu, L., Spiver, R.L., Tungate, F.L., Davis, B.H., *Fuel Sci. Technol. Int.* 14 (1996) 1337.
53. Srivastava, R.D., McIlvried, H.G., Winslow, J.C., Venktaraman, V.K., and Driscoll, D.J., "Proceedings of the Fifteenth Annual International Pittsburgh Coal Conference", Pittsburgh, PA, September 14, 1998.
54. Srivastava, R.D., Rao, V.U.S., Cinquegrane, G., and Stiegel, G.J., *Hydrocarbon Processing*, 1990.
55. Stiles, A.B., *Catalyst Manufacture*, Marcel Dekker, Inc., New York, 1983.

56. Sudsakorn, K., Goodwin Jr., J.G., Jothimurugesan, K., Adeyiga, A.A., *Ind. Eng. Chem. Res.*, 40 (2001) 4778.
57. Ward, A.D., and Ko, E.I., *Ind. Eng. Chem. Res.*, 34, 421 (1995).
58. Wei, D., Goodwin Jr., J.G., Oukaci, R., Singleton, A.H., *Appl. Catal. A* 210 (2001) 137.
59. Zaroachak, M.F., and McDonald, M.A., in Seventh DOE Indirect Liquefaction Contractors Meet Proc., Pittsburgh, Dec. 7-9, p. 96 (1987).
60. Zhao, R., Goodwin Jr., J.G., Jothimurugesan, K., Gangwal, S.K., Spivey, J.J., *Ind. Eng. Chem. Res.* 40 (2001) 1065.
61. Zhao, R., Goodwin Jr., J.G., Jothimurugesan, K., Gangwal, S.K., Spivey, J.J., *Ind. Eng. Chem. Res.* 40 (2001) 1320.
62. Zhao, R., Goodwin Jr., J.G., Oukaci, R., *Appl. Catal. A* 189 (1999) 99.
63. Zhao, R., Sudsakorn, K., Goodwin Jr., J.G., Jothimurugesan, K., Ganwal, S.K., Spivey, J.J., Spivey, J.J., *Cat. Today*, 71 (2002) 319.

**APPENDIX A:  
ATTRITION INDEX CALCULATIONS**

**Weight Percentage of Fines Lost**

“Weight percentage of fines lost” was basically the percentage ratio of the weight of fines ( $W_f$ ) collected by thimble, installed at the jet cup exit, and the weight of the total particles recovered ( $W_r$ ) in the jet cup at the end of an attrition test:

$$\begin{aligned} W_r = & \text{weight of fines generated } (W_f) \\ & + \text{weight of particles remaining at the bottom } (W_b) \end{aligned} \quad (\text{A-1})$$

$$\text{Weight percentage of fines lost (\%)} = \frac{W_f}{W_r} \times 100 \quad (\text{A-2})$$

**Net Change in Volume Moment**

“Net change in volume moment” was the percentage ratio of the difference of volume moments ( $X_{VM}$ ) before and after attrition test and the volume moment before attrition test:

$$\text{Net change in volume moment (\%)} = \frac{(X_{VM, \text{before attrition}} - X_{VM, \text{after attrition}})}{X_{VM, \text{before attrition}}} \times 100 \quad (\text{A3})$$

$$\text{Volume moment } (X_{VM}) = \frac{\sum X^4 dN}{\sum X^3 dN} \quad (\text{A-4})$$

Where  $N$  is the number of particles of size  $X$ .

**APPENDIX B:  
FE REDUCIBILITY CALCULATION**

The Fe reducibility by H<sub>2</sub> TPR was calculated based on the following assumptions:

- Assumption: 1) all Fe in a calcined Fe catalyst is in form of Fe<sub>2</sub>O<sub>3</sub>.  
2) all Cu and K in the catalyst are in the form of CuO and K<sub>2</sub>O, respectively.  
3) Fe<sub>2</sub>O<sub>3</sub> reacts with H<sub>2</sub> as:  $\text{Fe}_2\text{O}_3 + 3 \text{H}_2 = 2 \text{Fe} + 3 \text{H}_2\text{O}$ . (B-1)

Example: Calculation of Fe reducibility for 100 Fe/5Cu/4.2K/21SiO<sub>2</sub>

100 g or (100/55.8 = 1.8 mol) of Fe comes from (1.8/2 mol or 143.6 g of Fe<sub>2</sub>O<sub>3</sub>)

5 g or (5/63.5 = 0.08 mol) of Cu comes from 0.08 mol or 6.4 g of CuO)

4.2 g or 4.2/39.1 = 0.11 mol) of K comes from (0.08/2 mol or 10.4 g of K<sub>2</sub>O)

The weight of these components added to 21 g of SiO<sub>2</sub> gives the total catalyst weight of:

$$\text{Total catalyst wt.} = 143.6 + 6.4 + 10.4 + 21 = 181.4 \text{ g.}$$

Therefore, 1 g total calcined catalyst weight contains:

$$100/(55.8 * 181.4) = 0.01 \text{ mol of Fe or } 143.6/(159.6 * 181.4) = 0.005 \text{ mol of Fe}_2\text{O}_3$$

$$5/(63.5 * 181.4) = 4.3 * 10^{-4} \text{ mol of Cu}$$

$$4.2/(39.1 * 181.4) = 5.9 * 10^{-4} \text{ mol of K and}$$

$$21/(60.1 * 181.4) = 5.5 * 10^{-3} \text{ mol of SiO}_2.$$

From equation (B-1) mol Fe<sub>2</sub>O<sub>3</sub> consumes 3 \* 0.005 = 0.015 mol H<sub>2</sub>/g-cat. This amount of H<sub>2</sub> consumed represents 100% of Fe reducibility. The Fe reducibilities reported are the percentages of this amount.